

22011



National Library of Canada

Bibliothèque nationale du Canada

CANADIAN THESES ON MICROFICHE

THÈSES CANADIENNES SUR MICROFICHE

NAME OF AUTHOR/NOM DE L'AUTEUR Peter W. Wright

TITLE OF THESIS/TITRE DE LA THÈSE Electron Tunnelling into Superconductive Lead-Indium Alloys Subjected to Hydrostatic Pressure

UNIVERSITY/UNIVERSITÉ of Alberta

DEGREE FOR WHICH THESIS WAS PRESENTED / GRADE POUR LEQUEL CETTE THÈSE FUT PRÉSENTÉE PH.D.

YEAR THIS DEGREE CONFERRED/ANNÉE D'OBTENTION DE CE DEGRÉ Fall 1974

NAME OF SUPERVISOR/NOM DU DIRECTEUR DE THÈSE _____

Permission is hereby granted to the NATIONAL LIBRARY OF CANADA to microfilm this thesis and to lend or sell copies of the film.

L'autorisation est, par la présente, accordée à la BIBLIOTHÈQUE NATIONALE DU CANADA de microfilmer cette thèse et de prêter ou de vendre des exemplaires du film.

The author reserves other publication rights, and neither the thesis nor extensive extracts from it may be printed or otherwise reproduced without the author's written permission.

L'auteur se réserve les autres droits de publication, ni la thèse ni de longs extraits de celle-ci ne doivent être imprimés ou autrement reproduits sans l'autorisation écrite de l'auteur.

DATED/DATÉ SEPT 5 1974 SIGNED/SIGNÉ P. Wright

PERMANENT ADDRESS/RÉSIDENCE FIXÉ 7517-368 AVE, T6K 0L4 EDMONTON

THE UNIVERSITY OF ALBERTA

ELECTRON TUNNELLING INTO SUPERCONDUCTIVE LEAD-INDIUM ALLOYS
SUBJECTED TO HYDROSTATIC PRESSURE

by



PETER W. WRIGHT

A THESIS

SUBMITTED TO THE FACULTY OF GRADUATE STUDIES AND RESEARCH
IN PARTIAL FULFILMENT OF THE REQUIREMENTS FOR THE DEGREE
OF DOCTOR OF PHILOSOPHY

DEPARTMENT OF PHYSICS

EDMONTON, ALBERTA

FALL, 1974

THE UNIVERSITY OF ALBERTA
FACULTY OF GRADUATE STUDIES AND RESEARCH

The undersigned certify that they have read, and recommend to the Faculty of Graduate Studies and Research, for acceptance, a thesis entitled, ELECTRON TUNNELLING INTO SUPERCONDUCTIVE LEAD-INDIUM ALLOYS SUBJECTED TO HYDROSTATIC PRESSURE, submitted by PETER W. WRIGHT in partial fulfilment of the requirements for the degree of Doctor of Philosophy.

John Frank
.....
Supervisor

A. B. Capu
.....

J. S. R...
.....

A. D. H...
.....

C. R. James
.....

Jules Flabotte
.....
External Examiner

Date JULY 29 1974.....

TO VIOLET, WILLIAM, JANET & ANGELA

ABSTRACT

An investigation of the physical properties of the superconductive lead-indium alloy system has been carried out as a function of hydrostatic pressure, the results of which are presented in this thesis.

Samples were prepared in the form of tunnel junctions using standard vacuum deposition techniques from extremely high purity source elements. Pressure was applied to the samples by suspending them in a bath of solid helium and their conductance characteristics, through which most of the information was gained, were recorded using phase sensitive harmonic detection techniques. The chemical composition of the particular alloys investigated ($\text{Pb}_{88}\text{In}_{12}$ and $\text{Pb}_{64}\text{In}_{36}$) was determined using residual resistance ratio methods.

The pressure dependence of the energy gap and transition temperature were studied and found to be in excellent agreement with the recent data of Hansen et al (1973) and Galkin et al (1973).

The superconducting energy gap was found to decrease at a greater rate than the transition temperature indicating a trend towards weaker coupling. The magnitude of this trend was determined and found to be in good agreement with the theoretical prediction of Trofimenkoff and Carbotte (1970).

The pressure dependence of the principle phonon peaks of the system was also investigated including the localised mode first observed by Rowell et al (1965), and the corresponding Grüneisen mode gammas for these peaks calculated. Further information

regarding the pressure dependence of the phonon spectrum was obtained using the McMillan inversion programme (1965) for the $\text{Pb}_{64}\text{In}_{36}$ alloy. Data extracted by this process were used in conjunction with the McMillan equation for T_c (1968) from which fairly good agreement of the predicted pressure dependence of T_c with the directly obtained experimental value was in evidence.

By combining existing experimental data on the density of states at the Fermi surface with experimental results obtained here for the re-normalisation function, the pressure dependence of the band structure density of states has been derived. The values so obtained are in obvious disagreement with that of the free electron gas. Based on existing experimental evidence (Anderson and Gold (1965) and Anderson et al (1966)) and simple assumptions therefore, a value for the pressure dependence of the band structure density of states at the Fermi surface has been derived for the case of pure lead (which is not expected to differ greatly from the case at hand).

The use of tunnel junctions as sensitive pressure monitoring devices is strongly advocated. Their response to pressure has been found to be sensitive and reproducible while being almost independent of temperature.

ACKNOWLEDGEMENTS

I would like to extend my sincerest thanks to Dr. J.P. Franck who in supervising this research has provided inspiration and help while at the same time allowing me the freedom to pursue my own ideas.

A vote of thanks is also extended to Allan O'Shea who provided technical expertise that was second to none.

I am thankful to the Physics Department for their services and financial support. In the latter regard I would also like to gratefully acknowledge the financial support of the National Research Council of Canada.

Janet has done a tremendous job on the typing. Without her by my side I would have been beside myself.

TABLE OF CONTENTS

CHAPTER		PAGE
I	INTRODUCTION	1
II	THEORETICAL CONSIDERATIONS	3
	1. Towards the Microscopic Theories of B.C.S. and Bogoliubov	3
	2. The B.C.S. Hamiltonian	5
	3. The Bogoliubov Valatin Formalism	8
	4. The Superconducting Ground State and Energy Gap ($T = 0$)	16
	5. Finite Temperature Considerations and the Transition Temperature	20
	6. Theory of Tunnelling and the Density of States	23
	7. Strong Coupling Theory	29
	8. Observation of Phonon Structure by Tunnelling	36
	9. The Localised Mode	37
III	EXPERIMENTAL APPARATUS	40
	1. The Cryostat	40
	2. The Bomb	44
	3. Sample Housing and Holder	47
	4. High Pressure Production and Measurement	49
	5. The High Pressure Electrical Feedthrough	50

CHAPTER		PAGE
III	6. Vacuum Deposition	54
	7. Temperature Measurement	55
IV	ELECTRONIC DETECTION TECHNIQUES	56
	1. The Principle of the Measurement	56
	2. Detection of the Harmonics	57
	3. Circuit Design Considerations	60
	4. The Constant Current Bridge	61
	5. The Constant Voltage Bridge	65
V	EXPERIMENTAL METHOD	68
	1. Sample Fabrication	68
	2. Mounting Procedure	69
	3. Validity Checks	70
	4. An Experimental Run	71
	5. Determination of Sample Composition	73
VI	EXPERIMENTAL RESULTS AND DISCUSSION	78
	1. Introduction	78
	2. Pressure Dependence of the Transition Temperature	79
	3. The Energy Gap and its Dependence on Pressure	83
	4. Pressure Dependence of the Phonon Spectrum	92
	a. Directly Observed Principle Phonon Characteristics	92
	b. Inversion of the Eliashberg Gap Equations	105

CHAPTER		PAGE
VI	5. The Tunnel Junction as a Pressure Sensing Device	117
	6. Pressure Dependence of the Density of States	130
VII	CONCLUSIONS	138
	BIBLIOGRAPHY	140

LIST OF TABLES

Table	Description	Page
1	Pressure Dependence of the Transition Temperature	80
2	Comparative Transition Temperatures (at Zero Pressure)	81
3	Pressure Dependence of the Energy Gap	87
4	Comparative Pressure Dependence of the Energy Gap	88
5	Relative Rate of Change of the Energy Gap and Transition Temperature	90
6	Pressure Dependence of the Principle Phonon Peaks	101
7	Comparative Pressure Dependence of the Principle Phonon Peaks	102
8	Grüneisen Gammas of the Predominant Phonon Modes	104
9	Grüneisen Gammas Calculated from the Data of Galkin et al (1973)	104
10	Parameters Obtained from the Inversion Programme	115
11	Temperature and Pressure Values Along Isochores of He ⁴ at 400 Bar Intervals Starting with the Pressure at 0 K	126
12	Pressure Values (in p.s.i.) Along Isochores of Fluid Helium	128
13	Pressure Dependence of the Density States (Per Unit Volume)	131

LIST OF FIGURES

Figure		Page
1	Cryostat	41
2	Energy Gap Region for a Pb Al Junction at ~1.2K	42
3	He ⁴ Phase Diagram	45
4	High Pressure Bomb	46
5	Sample Housing and Holder	48
6	High Pressure Feedthrough	51
7	Circuit Logic	58
8	Constant Current Bridge (and support systems)	62
9	Constant Voltage Bridge	63
10	Sweep Circuit	64
11	R(293)/R(4) Vs Indium Concentration	75
12	Gap Region for a Pb ₆₄ In ₃₆ Sample (T = 2.51)	85
13	Comparison with the B.C.S. Theory (P = 0)	94
14	Comparison with the B.C.S. Theory (P = 0)	95
15	First and Second Derivatives for a Pb ₆₄ In ₃₆ Sample (P = 0)	97
16	Conductance Vs Energy for a Pb ₈₈ In ₁₂ Sample	98
17	Conductance Vs Energy for a Pb ₆₄ In ₃₆ Sample	99
18	First and Second Derivatives (36 at %) in the Vicinity of the Localised Mode	100
19	Input to Inversion Programme for a Pb ₆₄ In ₃₆ Sample	108
20	Phonon Spectra of a Pb ₆₄ In ₃₆ Sample	109
21	Gap Function for a Pb ₆₄ In ₃₆ Sample	110

Figure		Page
22	Renormalisation Function for a $\text{Pb}_{64}\text{In}_{36}$ Sample	111
23	Zero Bias Tunnel Resistance Vs Pressure For a Typical $\text{Pb}_{64}\text{In}_{36}$ Sample (T~30K)	119
24	Zero Bias Tunnel Resistance Vs Pressure for a Typical $\text{Pb}_{88}\text{In}_{12}$ Sample (T~30K)	120
25	Tunnel Resistance vs Energy for a Typical $\text{Pb}_{64}\text{In}_{36}$ Sample - Press = 50,000 p.s.i.	123
26	Tunnel Resistance vs Energy for a Typical $\text{Pb}_{64}\text{In}_{36}$ Sample - Press = 800 p.s.i.	124

CHAPTER I

INTRODUCTION

The intent of the author in writing this chapter is to bridge the gap between the Table of Contents and the ensuing thesis material.

An attempt has been made in Chapter II to develop the theory which underlies only those aspects relevant to the understanding of the experimental measurements. The chapter begins therefore (after a very brief historical introduction to superconductivity) with an account of the theory leading up to the development of the superconducting transition temperature and energy gap for which a many body approach utilising the Bogoliubov-Valatin transformations has been chosen in favour of the original (and more usually employed) many body theory of Bardeen, Cooper and Schrieffer (1957), henceforth B.C.S. Frequent recourse is however made to the B.C.S. theory. The advantage of this choice is that it can be extended to encompass the theory of electron tunnelling which provided the analytical tool for the study at hand. Extension of the theory to cover the case of the so called strong coupling superconductors follows. The principle difference in the phonon spectrum of the alloys from that of pure lead is the existence of a localised mode of vibration. The final two sections of Chapter II consist firstly of an attempt to account for the observation of phonon processes through electron tunnelling and secondly a simplistic justification for the existence of the localised mode.

Chapters III and IV contain descriptions of the experimental apparatus employed, the latter being devoted entirely to the electronic detection systems (and their operation). Circuit analyses are presented verifying the linear response of the two bridge circuits that were used.

Experimental method is the subject of the fifth chapter.

In Chapter VI, with the exception of section five, ordering of the results (and discussion thereof) has been based on the experimental ease with which they were obtained and more importantly, on the dependence of subsequent sections upon their predecessors.

CHAPTER II

THEORETICAL CONSIDERATIONS

1. Towards the Microscopic Theories of B.C.S. and Bogoliubov

Before developing in detail the theory which underlies the measurements made, it is felt pertinent to very briefly acquaint the reader with some of the historical background leading up to the successful theories of Bardeen, Cooper and Schrieffer (1957) henceforth B.C.S. and of Bogoliubov (1958) the latter being, in the main, the basis of approach used thereafter.

The phenomenon of superconductivity was discovered in 1911 by K. Onnes whilst studying the electrical resistance of mercury at low temperatures when he noticed that at some particular temperature, the resistance of his specimen dropped to a value which he could not differentiate from zero. This temperature came to be known as the transition (or critical) temperature T_c and is probably the best known property characteristic of the superconducting state. Subsequent studies showed this state to exist in numerous metals and alloys and that it was reversible in the sense of other thermodynamic phase changes. Attempts to explain the physical basis for the existence of this new state were first proposed by Gorter and Casimir (1934) and by F. and H. London (1934-1935). Both of these models were of a phenomenological nature treating the electrons in the metal as two fluids, one component being ascribed the properties of normal electrons whilst the other gave rise to the superconducting properties. The

difference in the approaches was that Gorter and Casimir used a thermodynamical treatment whilst the London treatment was electrodynamic in nature.

The first big step towards an understanding of the superconducting state at the microscopic level was achieved by H. Fröhlich (1950) who proposed that the critical temperature of a superconductor was related to its isotopic mass according to $T \propto M^{-1/2}$ and thus indicating that the lattice was instrumental in the onset of superconductivity. In arriving at this result, Fröhlich had considered the interaction of electrons with the lattice (virtual phonon exchange) and concluded that if such interactions, which were attractive, could overcome the normal electrostatic repulsion between these electrons then the superconducting state would be realised. This attempt proved quantitatively inadequate but the lattice involvement had been arrived at which was the key to the eventual successful microscopic theories.

In 1956, Cooper showed that two electrons of opposite momenta and spin interacting via a momentum dependant potential formed a bound state above the Fermi surface if the interaction between them was attractive no matter how weak. At this time, evidence was growing suggesting the existence of an energy gap in the single particle electron density of states near the Fermi surface.

Based mainly on the mechanism proposed by Fröhlich and the refinements of Cooper, invoking the pair concept, an extensive and successful theory of the superconducting state was developed by Bardeen, Cooper and Schrieffer in 1957 and, using a different mathematical approach, by Bogoliubov in 1958 from which such properties as the transition

temperature and the suggested single particle energy gap naturally arose. These theories were later extended to describe the so called strong-coupling superconductors which were found to exhibit structure in the electronic density of states curve which could not be accounted for by either of the above mentioned theories. These and other deviations from the B.C.S. predictions have been attributed to the specific nature of the lattice involvement with superconductivity in which for some classes of superconductors the electron phonon interaction is weak and can be described by the B.C.S. or Bogoliubov theories whilst for others the interaction is strong and necessitates a different approach. That class of superconductors which can be adequately described by the theories of B.C.S. or Bogoliubov have therefore become known as weak coupling (or B.C.S.) superconductors as opposed to those in which the lattice involvement is more prominent which are known as strong-coupling superconductors.

2. The B.C.S. Hamiltonian

In an attempt to arrive at a pervasive theory for superconductivity the search leant towards finding an interaction between electrons which would be attractive since this would lead to a lowering of the total energy of the superconducting state with respect to that of the normal state as was being found experimentally. In view of the growing belief that the lattice was involved with the onset of superconductivity and with the success of the isotope effect, the Hamiltonian of Fröhlich (from which the isotope effect evolved) seemed an obvious starting

point for the development of the theory. This Hamiltonian may be written explicitly in the form

$$H_{Fr} = H_0 + \sum_{k s k' s' q} W_{k k' q} c_{k'+q, s'}^\dagger c_{k, s}^\dagger c_{k, s} c_{k' s'} \quad 2-1$$

where $W_{k k' q}$ is a matrix element of the form $\frac{|M_q|^2 \hbar \omega_q}{(\epsilon_k - \epsilon_{k-q})^2 - (\hbar \omega_q)^2}$ 2-2

H_0 represents the system of noninteracting electrons and phonons whilst the succeeding term represents the interaction of electrons with the lattice. In physical terms we may think of the interactive term as representing a self-energy associated with the electrons in the following way. An electron moving through the lattice distorts the lattice (ion sites), the lattice in turn then reacts on the electron due to its changed electrostatic field. As the electron passes by, the lattice is allowed to relax. Such distortions of the lattice are quantised in terms of phonons and we may therefore think of the electrons moving through the lattice constantly absorbing and re-emitting phonons. This surrounding of the electrons by phonons has given rise to the concept of "dressed" or "clothed" electrons. The ability of such a dressed electron to repel a second electron in its vicinity is therefore reduced by this positive screening effect and it is this reduction of its potential to repel that is referred to as the self-energy of the electron. It should be noted that the exchanged phonons are very short lived and that as a consequence of the uncertainty principle, energy need not be conserved in the process, to this end the phonons involved are virtual.

Fröhlich's proposal therefore was that the desired attractive interaction could be realised if this screening of the conduction

electrons by the positive ion lattice sites was such as to invoke an effective attractive force between electrons which was larger than their ability to repel each other as bare electrons. The lowering in total energy (condensation energy) associated with the superconducting phase change as predicted by this model turned out to be three or four orders of magnitude greater than that observed. It can be seen from 2-1 that the Fröhlich Hamiltonian included interactions between electrons of all momenta and either spin and was in fact the reason for the over estimate of the condensation energy.

A refinement proposed by Cooper in 1956 eventually led to an acceptable form for the Hamiltonian when he showed that if there was a net attraction between a pair of electrons just above the Fermi surface then they could form a bound state. He also showed that such electrons which could form this bound state by phonon mediation must be within an energy range $\pm \hbar \omega_q$ of the Fermi surface where $\hbar \omega_q$ is of the order of an average phonon energy of the metal, and that for maximum lowering of energy all such pairs must have the same total momentum. This model may be visualised as follows. One electron moving through the lattice distorts the lattice thereby emitting a phonon. The second electron in the vicinity is then affected by this disturbance (phonon absorption) as it propagates through the lattice. If the energy of the phonon which mediates the process is greater than the electronic energy change invoked thereby then the resulting interaction is attractive. Such pairs of electrons are referred to as Cooper pairs.

This pair concept was extended to the macroscopic occupation level by Bardeen, Cooper and Schrieffer who formulated a reduced

problem in which only pairs whose constituents had equal and opposite momentum were considered. This reduces the Fröhlich Hamiltonian to:-

$$H_{BCS} = \sum_{ks} \epsilon_k c_{ks}^\dagger c_{ks} - \frac{1}{2} \sum_{kk's} V_{kk's} c_{k's}^\dagger c_{-k's}^\dagger c_{-ks} c_{ks} \quad 2-3$$

where $V_{kk'} = -2W_{-k,k,k'-k} - U_{kk'}$ 2-4

$U_{kk'}$ is a screened Coulomb repulsion term added to the Fröhlich Hamiltonian of 2-1. If $V_{kk'}$ is positive then the electron-electron interaction is attractive.

It can be shown that the ground state energy described by this Hamiltonian is minimised if, in addition to pairing only electrons whose momenta are equal and opposite, we also require that such paired electrons have opposite spin. Thus by imposing this restriction and applying the convention that an operator preceded by a minus sign implies a spin down state whilst one with a positive sign implies a spin up state e.g. $c_k^\dagger \equiv c_{k'\uparrow}^\dagger$; $c_{-k'} \equiv c_{(-k')\downarrow}$, we can write the Hamiltonian of B.C.S. as

$$H_{BCS} = \sum_k \epsilon_k (c_k^\dagger c_k + c_{-k}^\dagger c_{-k}) - \sum_{kk'} V_{kk'} c_k^\dagger c_{-k'}^\dagger c_{-k} c_k \quad 2-5$$

It is at this juncture that we depart from the B.C.S. development and proceed instead to study the eigenvalues and eigenstates of this Hamiltonian according to the Bogoliubov method.

3. The Bogoliubov Valatin Formalism

We next proceed to diagonalise the Hamiltonian given by 2-5 by first introducing a transformation to a new operator system defined by:-

$$\left. \begin{aligned}
 \gamma_k &= u_k c_k - v_k c_{-k}^\dagger & \gamma_{-k} &= u_k c_{-k} + v_k c_k^\dagger \\
 \text{and their conjugates} & & & \\
 \gamma_k^\dagger &= u_k c_k^\dagger - v_k c_{-k} & \gamma_{-k}^\dagger &= u_k c_{-k}^\dagger + v_k c_k
 \end{aligned} \right\} \quad 2-6$$

u and v are chosen to be real constants related by the condition

$$u_k^2 + v_k^2 = 1 \quad 2-7$$

Such a choice ensures that the newly defined operators satisfy the Fermi anticommutation laws namely:-

$$[A_p^\dagger, A_q^\dagger]_+ = [A_p, A_q]_+ = 0 \quad [A_p, A_q^\dagger]_+ = \delta_{pq} \quad 2-8$$

where the A represents either the newly created operators or the traditional electron (c type) annihilation and creation operators.

In order to justify the relationship 2-7 one such commutation relation for the new operator system is shown here.

$$\begin{aligned}
 [\gamma_k, \gamma_k^\dagger] &= (u_k c_k - v_k c_{-k}^\dagger)(u_k c_k^\dagger - v_k c_{-k}) + (u_k c_k^\dagger - v_k c_{-k})(u_k c_k - v_k c_{-k}^\dagger) \\
 &= u_k^2 [c_k, c_k^\dagger]_+ - u_k v_k [c_k, c_{-k}]_+ - u_k v_k [c_{-k}^\dagger, c_k^\dagger]_+ + v_k^2 [c_{-k}^\dagger, c_{-k}]_+ \\
 &= u_k^2 + v_k^2 \equiv 1 \quad \text{using assumption 2-7}
 \end{aligned}$$

The inverses of the B.V. transformations are easily obtained in the following form:-

$$\left. \begin{aligned}
 c_k &= u_k \gamma_k + v_k \gamma_{-k}^\dagger & c_k^\dagger &= u_k \gamma_k^\dagger + v_k \gamma_{-k} \\
 c_{-k} &= u_k \gamma_{-k} - v_k \gamma_k^\dagger & c_{-k}^\dagger &= u_k \gamma_{-k}^\dagger - v_k \gamma_k
 \end{aligned} \right\} \quad 2-9$$

We next proceed to transform the B.C.S. Hamiltonian to our new operator system. Writing 2-5 as the sum of kinetic and interaction terms we have:-

$$H_{BCS} = H_T + H_V = H_{BV} \text{ (in the transformed system)}$$

2-10

Considering first the term H_T , we have:-

$$\begin{aligned} H_T &= \sum_k \epsilon_k (c_k^\dagger c_k + c_{-k}^\dagger c_{-k}) \\ &= \sum_k \epsilon_k \{ (u_k \gamma_k^\dagger + v_k \gamma_{-k}) (u_k \gamma_k + v_k \gamma_{-k}^\dagger) + (u_k \gamma_{-k}^\dagger - v_k \gamma_k) \\ &\quad \times (u_k \gamma_{-k} - v_k \gamma_k^\dagger) \} \\ &= \sum_k \epsilon_k [u_k^2 \gamma_k^\dagger \gamma_k + v_k^2 \gamma_{-k}^\dagger \gamma_{-k} + u_k v_k (\gamma_k^\dagger \gamma_{-k}^\dagger + \gamma_{-k} \gamma_k) + v_k^2 \gamma_k \gamma_k^\dagger + \\ &\quad u_k^2 \gamma_{-k}^\dagger \gamma_{-k} - u_k v_k (\gamma_{-k}^\dagger \gamma_k^\dagger + \gamma_k \gamma_{-k})] \end{aligned}$$

2-11

For simplicity we write this expression term by term as

$$H_T \equiv \sum_k \epsilon_k [P + Q + R + S + T + U] \text{ then using the anticommutation laws}$$

for the γ

$$R + U = 2u_k v_k (\gamma_k^\dagger \gamma_{-k}^\dagger + \gamma_{-k} \gamma_k)$$

$$Q = v_k^2 \gamma_{-k}^\dagger \gamma_{-k} = v_k^2 (1 - \gamma_{-k}^\dagger \gamma_{-k})$$

$$S = u_k^2 \gamma_k^\dagger \gamma_k = u_k^2 (1 - \gamma_k^\dagger \gamma_k)$$

$$P + S = v_k^2 + (u_k^2 - v_k^2) \gamma_k^\dagger \gamma_k$$

$$T + Q = v_k^2 + (u_k^2 - v_k^2) \gamma_{-k}^\dagger \gamma_{-k}$$

before re-collecting these terms, new number operators are defined

for the gammas in analogy with the electron number operators i.e.

$$\gamma_k^\dagger \gamma_k \equiv m_k \quad \text{and} \quad \gamma_{-k}^\dagger \gamma_{-k} \equiv m_{-k}$$

We can thus write H_T in the following way,

$$H_T = \sum_k \epsilon_k [(P + S + T + Q) + (R + U)]$$

to get:-

$$H_T = \sum_k \epsilon_k [2v_k^2 + (u_k^2 - v_k^2)(m_k + m_{-k}) + 2u_k v_k (\gamma_k^\dagger \gamma_{-k}^\dagger + \gamma_{-k} \gamma_k)] \quad 2-12$$

The interaction term H_V of equation 2-10 is treated in a similar fashion (more extensive use is made of the commutation relations and the grouping of terms requires greater insight due to the complexity of this term) to yield

$$H_V = - \sum_{kk'} V_{kk'} [u_k v_k u_{k'} v_{k'} (1 - m_k - m_{-k})(1 - m_{k'} - m_{-k'}) + u_k v_k (1 - m_k - m_{-k})(u_{k'}^2 - v_{k'}^2)(\gamma_{-k'} \gamma_{k'} + \gamma_{k'}^\dagger \gamma_{-k'}^\dagger)] +$$

(fourth order off diagonal terms) 2-13

The Hamiltonian is now diagonalised for the ground state of the superconductor for which we assume that all the occupation numbers such as m_k vanish. This is achieved by requiring that the sum of off diagonal contributions to H_{BV} from H_T and H_V cancel one another i.e.

$$\sum_k 2\epsilon_k u_k v_k (\gamma_k^\dagger \gamma_{-k}^\dagger + \gamma_{-k} \gamma_k) - \sum_{kk'} V_{kk'} u_k v_k (u_{k'}^2 - v_{k'}^2) (\gamma_{k'}^\dagger \gamma_{-k'}^\dagger + \gamma_{-k'} \gamma_{k'}) = 0 \quad 2-14$$

in which the assumption is made that the expectation value of the fourth order off diagonal elements is negligible in the ground state of the system. Elimination of the off diagonal elements in this manner enables us to consider the system as being composed of independent fermions. Considering equation 2-14 term by term we get:-

$$2\epsilon_k u_k v_k - (u_k^2 - v_k^2) \sum_{k'} V_{kk'} u_{k'} v_{k'} = 0 \quad 2-15$$

which dictates the form that u and v (the B.V. transformation) must have to be consistent with the diagonalisation condition. Since u and v are interrelated they may be defined in terms of a single

parameter as follows:-

$$u_k = (\frac{1}{2} - x_k)^{\frac{1}{2}} \quad \text{and} \quad v_k = (\frac{1}{2} + x_k)^{\frac{1}{2}} \quad 2-16$$

Equation 2-15 then becomes

$$2\varepsilon_k (\frac{1}{4} - x_k^2)^{\frac{1}{2}} + 2x_k \Delta_k \quad 2-17$$

where we have introduced a new quantity defined by:-

$$\Delta_k = \sum_{k'} V_{kk'} (\frac{1}{4} - x_{k'}^2)^{\frac{1}{2}} \quad 2-18$$

$$\text{Thus } x_k = \frac{\pm \varepsilon_k}{2(\varepsilon_k^2 + \Delta_k^2)^{\frac{1}{2}}} \quad 2-19$$

substitution for x_k in 2-18 yields a form for Δ_k :-

$$\Delta_k = \frac{\frac{1}{2} \sum_{k'} V_{kk'} \Delta_{k'}}{(\varepsilon_{k'}^2 + \Delta_{k'}^2)^{\frac{1}{2}}} \quad 2-20$$

This latter equation represents an integral equation which can in principle be solved if we know the form of the interaction potential $V_{kk'}$. In order to conserve the total number of particles in the system we must choose the Fermi surface as the zero level of energy for the system. The proof of this is seen below which also enables us to decide upon the sign in equation 2-19. The number of electrons in the system is given by:-

$$N = \sum_k (c_k^\dagger c_k + c_{-k}^\dagger c_{-k})$$

The expectation value of N is, using equation 2-12:-

$$\begin{aligned} \langle 0 | N | 0 \rangle &= N \langle 0 | 0 \rangle = \langle N \rangle = \sum_k \langle 0 | 2v_k^2 | 0 \rangle + \langle 0 | (u_k^2 - v_k^2) \\ &\quad x(m_k + m_{-k}) | 0 \rangle + \langle 0 | 2u_k v_k (\gamma_k^\dagger \gamma_{-k}^\dagger + \gamma_{-k} \gamma_k) | 0 \rangle \end{aligned} \quad 2-21$$

Now for the ground state of the system the $m_k \equiv 0$ in the second term

whilst the third term can be shown to produce only zero eigenvalues by replacing the γ according to equation 2-6. Thus the expectation value of N reduces to:-

$$\langle N \rangle = \sum_k 2v_k^2 = \sum_k (1 + 2x_k) \quad 2-22$$

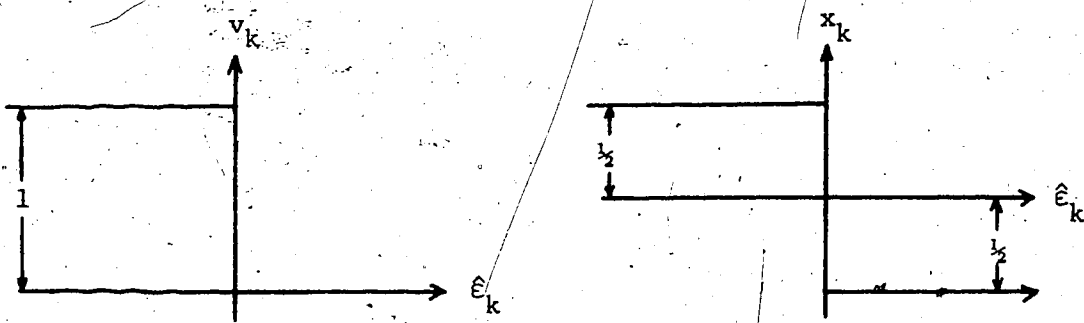
If we had no interactions i.e. all the electrons resided below the Fermi surface then we know that N must have the form

$$\langle N \rangle = \sum_{k < k_f} 2 \quad \text{and} \quad \langle N \rangle = 0 \quad \text{for} \quad k > k_f \quad 2-23$$

where the factor of two arises because of the dual spin nature of fermions. For the non interacting case then we must put $V_{kk'} \equiv 0$ and thus from equation 2-18, $\Delta_k \equiv 0$ also. By substitution then in equation 2-19, we see for the non interacting case that:-

$$x_k = \pm \frac{1}{2}$$

Where the positive sign is chosen to represent the system below the Fermi surface and the negative sign for above the Fermi surface thereby making equation 2-22 consistent with the real physical situation of equation 2-23. So for the normal metal the B.V. transformation has the form

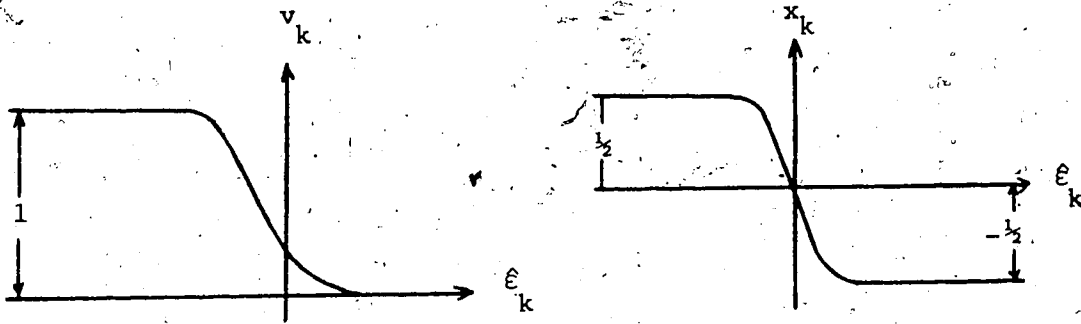


Where $\hat{\epsilon}_k$ here and henceforth will be used to denote measurements with respect to the Fermi surface. Turning attention now to the

interacting case ($V_{kk'} \neq 0$) of a superconductor we can see from equation 2-22 that for the number of particles to be conserved that x_k must be an odd function of $(\epsilon_k - \epsilon_F)$ as was the case above and thus we choose the negative sign for x_k and have therefore:-

$$x_k = -\frac{1}{2} \frac{\epsilon_k}{(\epsilon_k^2 + \Delta_k^2)^{1/2}} \quad 2-24$$

Notice that $V_{kk'} \rightarrow 0$ (and hence $\Delta_k \rightarrow 0$) has the highly desirable effect of encompassing the normal metal case. Equation 2-24 describes the form that the B.V. transformations (i.e. the restriction on our original u and v) must have for the Hamiltonian to be of diagonal form and are shown pictorially below.



Bardeen, Cooper and Schrieffer solved equation 2-20 for delta using a very simple potential for which they proposed the form

$$V_{kk'} = \begin{cases} V & \text{for } |\epsilon_k| \text{ \& } |\epsilon_{k'}| < \hbar\omega_D \\ 0 & \text{otherwise} \end{cases}$$

Expressed in integral form, equation 2-20 becomes

$$\Delta_k = \frac{1}{2} \int_{-\infty}^{\infty} D(\epsilon_{k'}) \frac{\Delta_{k'}}{(\epsilon_{k'}^2 + \Delta_{k'}^2)^{1/2}} V_{kk'} d\epsilon_{k'} \quad 2-25$$

Since v_{kk} is constant and so is $\hbar\omega_D$, (the Debye energy) then it follows that Δ_k is constant and we may therefore omit the subscripts and take V outside the integral. $D(\hat{\epsilon}_k)$ represents the density of electron states (for electrons of one spin) and is assumed constant at the Fermi surface thus equation 2-25 reduces to

$$= \frac{VD}{2} \int_{-\hbar\omega_D}^{\hbar\omega_D} \frac{\Delta}{(\hat{\epsilon}^2 + \Delta^2)^{1/2}} d\hat{\epsilon}$$

This integral can now be easily solved using the substitution

$\hat{\epsilon} = \Delta \sinh x$ to yield

$$\Delta = \hbar\omega_D / \{\sinh(1/DV)\} \quad 2-26$$

For a great many metals, estimates of the quantity (DV) yield values $\leq 10^{-1}$ whence it is easy to see from the definition of the hyperbolic function

$$\sinh x = \frac{1}{2}(e^x - e^{-x})$$

that we may reasonably make an approximation to 2-26 of

$$\Delta = 2\hbar\omega_D \exp[-1/DV(\epsilon_f)] \quad 2-27$$

Those metals for which the above approximation is valid are said to be weak-coupling superconductors. It can be seen from 2-27 that Δ is an extremely small quantity and that because of this the parameter x_k defined by equation 2-24 differs from $\pm \frac{1}{2}$ only very close (within $\pm\Delta$) of the Fermi surface. Examining this implication from a wider viewpoint we see that as a consequence of x_k having the values $\pm \frac{1}{2}$ in regions remote from the Fermi surface, the values of u and v become either unity or zero and hence from equation 2-6

we see that our newly introduced operators gamma revert back to a single c type operator as in the case of a normal metal.

We have to this point then built up a picture of a superconductor which resembles a normal metal, except within a small region bounding the Fermi surface where the electrons interact in a very specific manner. The nature of this interaction is the pair concept alluded to earlier and the gamma operators set forth at the beginning of this section are those which create and destroy such Cooper pairs. The term quasiparticle is used to describe a single electron while in a paired state. The parameter Δ is associated with the energy of formation (or destruction) of such pairs. It is the very small lowering of energy associated with the pairing of electrons combined with the fact that this pairing only occurs in a very restricted region at the Fermi surface that accounts so nicely for the experimentally observed small lowering of the total energy of the metal when in the superconducting state.

4. The Superconducting Ground State and Energy Gap (T = 0)

Having established in the previous section the condition that the off diagonal elements of $H_{BV} = H_T + H_V$ vanish, we are left with the diagonalised Hamiltonian

$$H_{BV} = \sum_k \epsilon_k [2v_k^2 + (u_k^2 - v_k^2)(m_k + m_{-k})] - \sum_{k,k'} V_{kk'} u_k v_{k'} u_{k'} v_k \\ (1 - m_{k'} - m_{-k'}) (1 - m_k - m_{-k})$$

2-28

which in the ground state where the $m \equiv 0$ reduces to

$$H_{BVG} = \sum_k 2\epsilon_k v_k^2 - \sum_{kk'} V_{kk'} u_k v_k u_{k'} v_{k'} \quad 2-29$$

The ground state wave function Ψ_0 for the superconductor must be an eigenfunction of the diagonalised Hamiltonian so that for all possible k :-

$$\gamma_k |\Psi_0\rangle = \gamma_{-k} |\Psi_0\rangle = 0 \quad 2-30$$

This in effect is an attempt to create a state lower than the ground state defined by Ψ_0 . In order to find the form of Ψ_0 the following argument is extended. Since the gammas obey the usual Fermi anti-commutation laws, products such as $\gamma_k \gamma_k = \gamma_{-k} \gamma_{-k} = 0$ and so equation 2-30 is satisfied by operating on the vacuum state with all of the possible products of the operators γ_k and γ_{-k} because such products would always contain a product of the type $\gamma_k \gamma_k$ and thereby yield a zero eigenvalue. For all possible k values therefore this may be stated as

$$|\Psi_0\rangle = \left(\prod_k \gamma_k \gamma_{-k} \right) |o\rangle = \left[\prod_k (u_k c_k - v_k c_{-k}^\dagger) (u_{-k} c_{-k} + v_{-k} c_k^\dagger) \right] |o\rangle \quad 2-31$$

where again use has been made of the original definition of the gammas. This expression simplifies by using the anticommutation relations and normalising throughout by the product of all of the v_k to give for the ground state wave function

$$|\Psi_0\rangle = \prod_k (u_k - v_k c_{-k}^\dagger c_k^\dagger) |o\rangle \quad 2-32$$

It is possible to justify the above expression on a purely mathematical basis in which we first propose the form for $|\Psi_0\rangle$ as given in 2-32 and show that it is consistent with the physical proposal of equation 2-30, the derivation for which will not be presented here.

Quasiparticle excitations of the system can be created simply by acting upon the ground state wave function with the creation operators γ_k^\dagger and γ_{-k}^\dagger .

The ground state energy of the superconducting state ϵ_s can be obtained by calculating the expectation value of the Hamiltonian given by equation 2-29.

$$\epsilon_s = \langle H_{BVG} \rangle = \langle 0 | \sum_k 2\hat{\epsilon}_k v_k^2 - \sum_{kk'} V_{kk'} u_k v_k u_{k'} v_{k'} | 0 \rangle$$

Using the model potential proposed by B.C.S. we see that all of the quantities in the above expression are constants and therefore

$$\epsilon_s = \sum_k 2\hat{\epsilon}_k v_k^2 - \sum_{kk'} V_{kk'} u_k v_k u_{k'} v_{k'} \quad 2-33$$

When excitations are present however ($m \neq 0$) we must revert to the Hamiltonian of equation 2-28 the terms of which may be rearranged to give

$$H_{BV} = \epsilon_s + \sum_k (m_k + m_{-k}) [(u_k^2 - v_k^2)\hat{\epsilon}_k + 2u_k v_k \sum_{kk'} V_{kk'} u_{k'} v_{k'}] + \text{higher order terms} \quad 2-34$$

and where use has been made of the expression derived for ϵ_s .

By substituting in equation 2-34 (using equations 2-16, 2-20 and 2-22) this expression can be rewritten in the form:-

$$H_{BV} = \epsilon_s + \sum_k (\hat{\epsilon}_k^2 + \Delta^2)^{1/2} (m_k + m_{-k}) + \dots \quad 2-35$$

It can now be seen that this represents a system whose ground state energy is given by ϵ_s and whose (quasiparticle) excitations are given by:-

$$E_k = (\hat{\epsilon}_k^2 + \Delta^2)^{1/2} \quad 2-36$$

These quasiparticles cannot be created singly since any physical

process is represented by at least two electron operators e.g. scattering, which results in two gamma type operators. The minimum energy required to create (or break up) such a pair of quasiparticles is 2Δ as can be seen from equation 2-36. When a Cooper pair is broken up one electron can be excited across the Fermi surface to a state $(\epsilon_f + \Delta)$ whilst the other falls back into the Fermi sea $(\epsilon_f - \Delta)$ until re-pairing with other electrons occurs. In this way the energy gap in the single particle electron density of states that is observed can be visualised.

In analogy with the density of states of a normal metal, the density of quasiparticle states for the superconductor can be deduced from

$$D(E) = \frac{dk}{dE} = \frac{d\hat{\epsilon}}{dE} \frac{dk}{d\hat{\epsilon}}$$

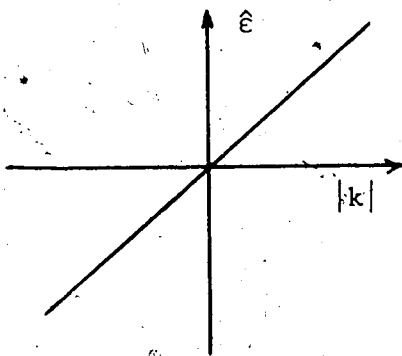
where $dk/d\hat{\epsilon}$ is the density of Bloch states of a normal metal.

Using equation 2-36 we find that:-

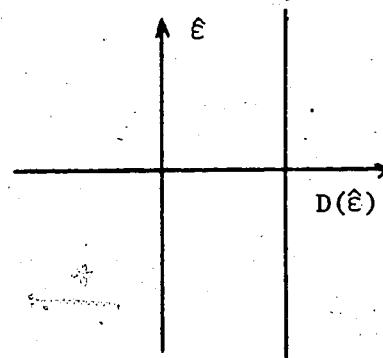
$$D(E) = \begin{cases} 2D(\epsilon_f) \frac{|E|}{(E^2 - \Delta^2)^{1/2}} & \text{for } |E| > \Delta \\ 0 & \text{for } |E| \leq \Delta \end{cases}$$

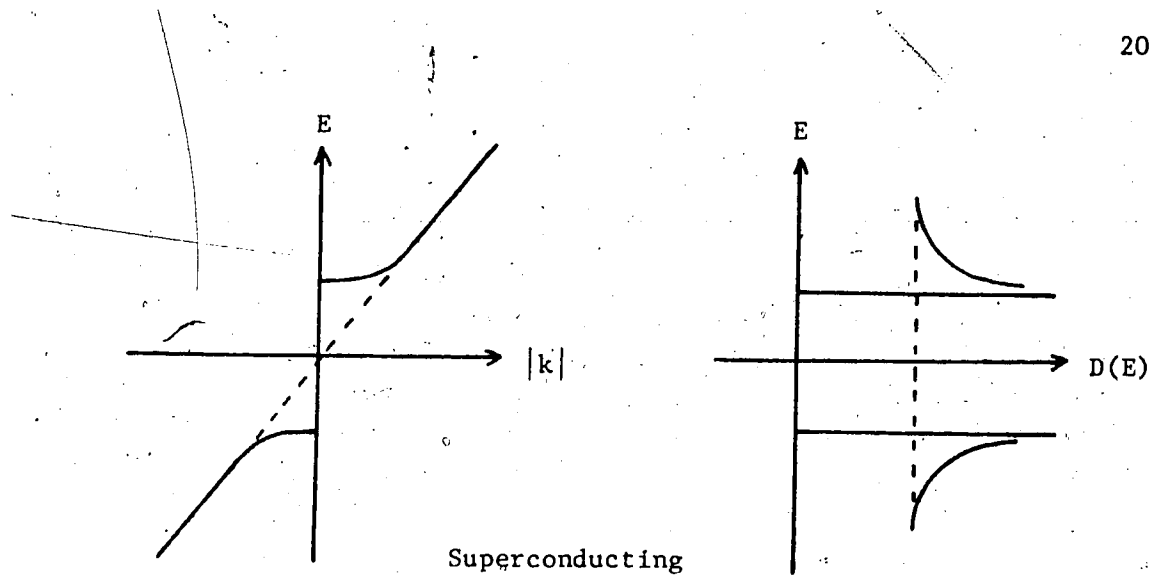
2-37

Pictorially this compares with the normal metal as below



Normal





5. Finite Temperature Considerations and the Transition Temperature

In the previous section it had been assumed that the number of quasiparticle excitations was very small, i.e. $\Delta \gg kT$, a situation we might envisage as $T \rightarrow 0$. We now treat the more physical case of $T \neq 0$ where we no longer assume the number of quasiparticle excitations to be negligible. In so doing we will arrive at a modified form for the quasiparticle excitation energies and energy gap, and derive an expression for the transition temperature. In proceeding, we assume that the Hamiltonian for the system can still be diagonalised (an assumption to be justified). We are left then with the Hamiltonian given by equation 2-28. The energy required to create a quasiparticle excitation will be given by:-

$$E_k = \frac{d\langle H_{BV} \rangle}{d\langle n_k \rangle} \quad 2-38$$

If we apply this to equation 2-28 we get

$$E_k = \hat{\epsilon}_k (u_k^2 + v_k^2) + 2u_k v_k \sum_{k'} V_{kk'} u_{k'} v_{k'} (1 - \langle n_{k'} \rangle - \langle n_{-k'} \rangle) \quad 2-39$$

In defining the excitation energies as in 2-38 we may treat the problem

as a system of independent fermions and obtain an approximate solution by replacing the m by their thermal averages according to Fermi-Dirac statistics.

$$\langle m_k \rangle = \langle m_{-k} \rangle = \frac{1}{\exp(E_k/kT) + 1} = f(E_k) \quad 2-40$$

The off diagonal terms are treated in exactly the same way as in the previous case ($T \rightarrow 0$) except that we do not now assume that the m vanish also, but rather they take the form of their thermal average as in equation 2-40. The resulting expression is:-

$$2\hat{\epsilon}_k u_k v_k - (u_k^2 - v_k^2) \sum_{k'} V_{kk'} u_{k'} v_{k'} [1 - 2f(E_{k'})] = 0 \quad 2-41$$

Comparing this with equation 2-15 we see that they differ only by the factor in the square brackets containing the Fermi function.

We define a modified gap function here which is temperature dependent:-

$$\Delta_k(T) = \sum_{k'} V_{kk'} (\frac{1}{2} - x_{k'}^2)^{\frac{1}{2}} [1 - 2f(E_{k'})] \quad 2-42$$

The development is now as for the case of $T \rightarrow 0$ (with the B.V. transformation x being temperature dependent) and leads to the integral gap equation for non zero T of:-

$$\Delta_k(T) = \frac{1}{2} \sum_{k'} V_{kk'} \frac{\Delta_{k'}(T)}{[\hat{\epsilon}_{k'}^2 + \Delta_{k'}^2(T)]^{\frac{1}{2}}} [1 - 2f(E_{k'})] \quad 2-43$$

By substituting into the expression for E_k (equation 2-39) as before and including the explicit form of the Fermi functions given by equation (2-40) we get for the quasiparticle energies

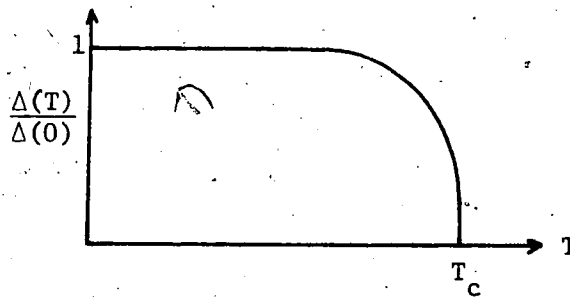
$$E_k = [\hat{\epsilon}_k^2 + \Delta^2(T)]^{\frac{1}{2}} \quad 2-44$$

This expression is exactly that obtained earlier but with the temperature dependent gap function.

Using the model potential of B.C.S. and solving as before the integral equation 2-43 for the gap we find that

$$VD(\epsilon_f) \int_0^{\hbar\omega_D} \frac{\tanh[(\epsilon^2 + \Delta^2)^{1/2}/2kT] d\epsilon}{(\epsilon^2 + \Delta^2)^{1/2}} = 1 \quad 2-45$$

This clearly is a very complicated implicit expression for the energy gap at finite temperature. It can be seen however that as T increases, the numerator decreases and therefore for the left hand side of this expression to remain constant equal to unity, the denominator must decrease also. This implies therefore that Δ is a monotonically decreasing function of temperature. Such is the case observed experimentally as shown below; typically



It is very satisfying that if $T \equiv 0$ then this expression yields identically the previous expression derived.

To obtain an expression for the transition temperature we need to impose the condition that $\Delta \rightarrow 0$ as $T \rightarrow T_c$ in this integral which can then be performed to yield:-

$$kT_c = 1.14\hbar\omega_D \exp[-1/VD(\epsilon_f)]$$

2-46

having made use of the weak coupling approximation $kT_c \ll \hbar\omega_D$.

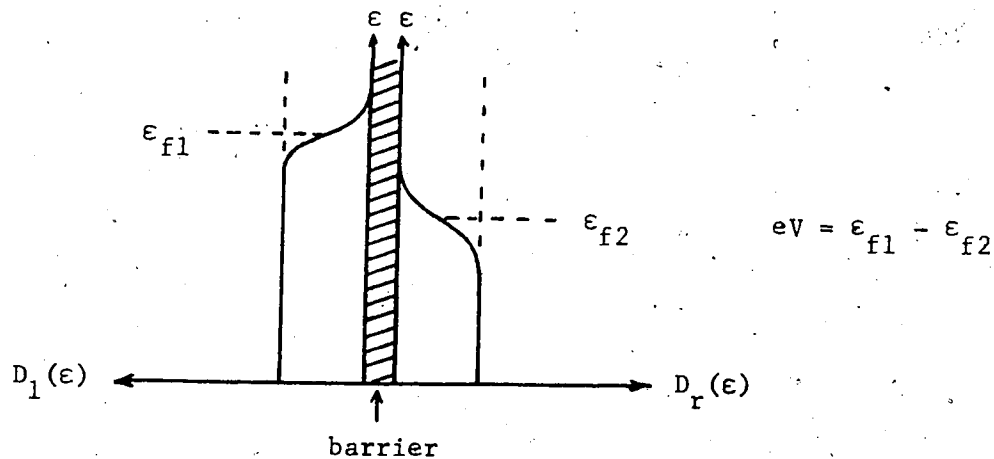
Recalling the expression for the $T = 0$ case for $\Delta(0)$ (equation 2-27) and comparing with this we have that, for the simple constant potential model of B.C.S. in the weak coupling assumption:-

$$\frac{2\Delta(0)}{kT_c} = 3.53 \quad \text{UNIVERSALLY} \quad 2-47$$

This key result is often used experimentally as an expression of the weak coupling approximation.

6. Theory of Tunnelling and the Density of States

Consideration is now given to the transport of electrons across an insulating barrier. This might be represented by the diagram below for the case when both metals are in the normal state,



where the Fermi level energy of metal one has been raised by an amount eV with respect to that of metal two. The quantities $D_1(\epsilon)$ and $D_r(\epsilon)$ represent the density of electron states in metals one and two respectively. Notice that in accordance with the diagram on page 19 that the dotted line represents the density of available

states in a normal metal whilst the shaded region represents the density of occupied states as obtained by multiplying the $D(\epsilon)$ by the respective Fermi function.

A Hamiltonian representing this system may be written as the sum of three terms the first of which describes those electrons of metal one on the left hand side and the second for those on the right whilst the third is a term relating to the transfer of electrons from side to side. Thus:-

$$H = \sum_{ks} \epsilon_k c_{ks}^\dagger c_{ks} + \sum_{ks} \epsilon_k d_{ks}^\dagger d_{ks} + \sum_{kk's} T_{kk'} (c_{ks}^\dagger d_{k's} + d_{k's}^\dagger c_{ks}) \quad 2-48$$

Since it is proposed here to calculate the net tunnel current we need only concern ourselves with the third term of this expression.

The transition probability in lowest order is given by

$$|T_{kk'}|^2 = |T|^2.$$

Because of the applied potential difference V , the energy of electrons of metal one are raised in energy by an amount eV . These electrons of energy $\hat{\epsilon}_k$ can then be elastically scattered (tunnel) to an available state k' in metal two whose energy is given by $(\hat{\epsilon}_k + eV)$, in this way energy is conserved. A similar argument applies to tunnelling in the opposite direction. The net flow of electrons from left to right is therefore proportional to:-

$$\sum_{kk's} |T|^2 [f_k (1 - f_{k'}) - f_{k'} (1 - f_k)] \delta(\hat{\epsilon}_{k'} - \hat{\epsilon}_k - eV) \quad 2-49$$

where the f_k represent the probability of occupancy of a given state k . Expression 2-49 may be interpreted physically if we associate f_k with the probability that the state k from which an

electron originates is occupied and $(1 - f_{k'})$ with the probability that the state k' to which it tunnels is unoccupied, energy conservation being accounted for by the delta function. The tunnel current therefore may be obtained from expression 2-49 by putting it in integral form:-

$$I_{NN} \propto T^2 \{f(\hat{\epsilon}_k) - f(\hat{\epsilon}_k + eV)\} D(\hat{\epsilon}_k) D(\hat{\epsilon}_k + eV) d\hat{\epsilon}_k \quad 2-50$$

In obtaining this we have complied explicitly with the energy conservation aspect. T^2 is taken to be the square of some average tunnelling matrix element. If we were to proceed from this point using the phenomenological approach we would assume that T^2 and D^2 (arising from the density of states product) were constant and extricate them from the integral, here however a brief explanation is given to justify this procedure. Using the particle in a box concept of tunnelling across a narrow potential barrier it can be shown fairly easily that the element T is given by:-

$$T = Ak + B \quad 2-51$$

A and B being constants and k being the wave vector in the direction that tunnelling takes place. The kinetic energy $\hat{\epsilon}_k$ associated with the state k is simply

$$\hat{\epsilon} = \frac{\hbar^2 k^2}{2m} - \epsilon_f \Rightarrow \frac{d\hat{\epsilon}}{dk} = \frac{\hbar^2 k}{m} \quad 2-52$$

Thus we see from 2-51 and 2-52

$$T \propto \frac{d\hat{\epsilon}}{dk} \quad 2-53$$

$$\text{But } D(\hat{\epsilon}) = \frac{dN}{d\hat{\epsilon}} = \frac{dN}{dk} \frac{dk}{d\hat{\epsilon}} \quad 2-54$$

and we can see therefore that the energy dependence of the product

$\frac{dN}{dk}$ in the integral disappears. If we make the justifiable assumption that dN/dk is constant in the region of the Fermi surface we have for I that

$$I_{NN} \propto D_1(\epsilon_f) D_r(\epsilon_f) T^2 \int \{f(\hat{\epsilon}_k) - f(\hat{\epsilon}_k + eV)\} d\hat{\epsilon}_k \quad 2-55$$

This model is consistent with the premise that tunnelling takes place at or near the Fermi surface and that $\epsilon_f \gg eV$.

The factor $f(\hat{\epsilon}_k + eV)$ in equation 2-55 can now be expanded as a Taylor series about $\hat{\epsilon}_k$ whereupon after neglecting terms containing powers of (eV) squared and greater we have:-

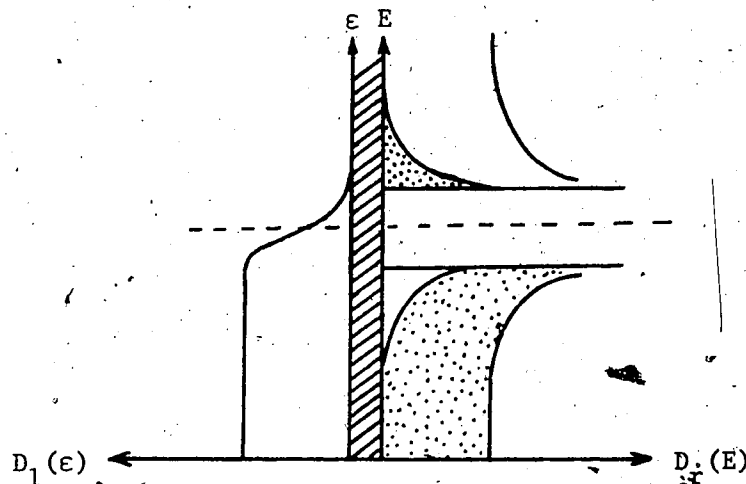
$$I_{NN} \propto D_1(\epsilon_f) D_r(\epsilon_f) T^2 \int eV f'(\hat{\epsilon}_k) d\hat{\epsilon}_k$$

At low temperatures, f approximates to a delta function giving:-

$$I_{NN} \propto D_1(\epsilon_f) D_r(\epsilon_f) T^2 eV \quad 2-56$$

For N - N (normal metal - normal metal) tunnelling thus, an ohmic dependence is predicted.

Attention is now turned to the case where one of the metals is in the superconducting state as depicted below.



Once again, in an effort to derive an expression for the tunnel current, we need consider only the tunnelling term of the Hamiltonian of equation 2-48 except that those operators previously assigned as d for states on the right hand side (metal two) must now be replaced by their quasiparticle counterparts in keeping with the B.V. formalism adopted earlier. Explicitly we have then:-

$$H_T = \sum_{kk'} T [c_k^\dagger (u_k \gamma_k + v_k \gamma_{-k}^\dagger) + c_{-k}^\dagger (u_k \gamma_{-k} - v_k \gamma_k^\dagger) + (u_k \gamma_k^\dagger + v_k \gamma_{-k}) c_k + (u_k \gamma_{-k}^\dagger - v_k \gamma_k) c_{-k}] \quad 2-57$$

Notice that the spin has been included explicitly here in keeping with the pair concept and has therefore been omitted from the summation sign, it is also very relevant to recall that if the interaction potential $V_{kk'}$, responsible for the pairing tends to zero then the γ 's revert to single electron operators and we have identically the preceding case for N - N tunnelling.

The physical interpretation of equation 2-57 is as follows. The first term creates an electron on the left hand side of the barrier and either creates or destroys a quasiparticle excitation on the right (above or below the Fermi surface). The other terms may be interpreted in an analogous manner.

For a term such as $c_k^\dagger \gamma_k$, to cause a real scattering (tunnelling) we must have that $E_{k'} = \hat{\epsilon}_k + eV$ for an applied potential V . Note that in this case we are measuring energies with respect to the Fermi surface as was the case in our previous application of the B.V. formalism. Similarly for the term $c_{-k}^\dagger \gamma_{-k}^\dagger$, to cause a real scattering process we must have $-\hat{\epsilon}_k - eV = E_{k'}$.

Extending this type of argument to the remaining terms in 2-57 and proceeding as with the N - N case we get:-

$$I_{NS} \propto \sum_{kk'} |T|^2 (u_{k'}^2 \{f(\hat{\epsilon}_k) [1 - f(E_{k'})] - f(E_{k'}) [1 - f(\hat{\epsilon}_k)]\} \delta(E_{k'} - \hat{\epsilon}_k - eV) + v_{k'}^2 \{f(\hat{\epsilon}_k) f(E_{k'}) - [1 - f(\hat{\epsilon}_k)] [1 - f(E_{k'})]\} \delta(\hat{\epsilon}_k + E_{k'} + eV)) \quad 2-58$$

having grouped together terms in u^2 and v^2 . By multiplying out, collecting terms and expressing in integral form we have

$$I_{NS} \propto \int T^2 D(\hat{\epsilon}_k) D(E = \hat{\epsilon}_k + eV) \{u_{k'}^2 [f(\hat{\epsilon}_k) - f(\hat{\epsilon}_k + eV)] + v_{k'}^2 [f(\hat{\epsilon}_k) - 1 + f(-\hat{\epsilon}_k - eV)]\} d\hat{\epsilon}_k \quad 2-59$$

where the f functions have been included explicitly. Since the metal on the right hand side of the barrier is a superconductor, the density of states function $D(E)$ has the form given by equation 2-37. This expression can be further reduced by noticing that $f(-E) = 1 - f(E)$ to give:-

$$I_{NS} \propto \int T^2 D(\hat{\epsilon}_k) D(\hat{\epsilon}_k + eV) \{f(\hat{\epsilon}_k) [u_{k'}^2 + v_{k'}^2] - f(\hat{\epsilon}_k + eV) \times [u_{k'}^2 + v_{k'}^2]\} d\hat{\epsilon}_k \quad 2-60$$

According to the original B.V. assumption $u^2 + v^2 = 1$ hence we have

(replacing $D(\hat{\epsilon}_k + eV)$ using 2-37) that:-

$$I_{NS} \propto T^2 D_1(\epsilon_F) D_r(\epsilon_F) \int \frac{|E|}{(E^2 - \Delta^2)^{1/2}} [f(\hat{\epsilon}_k) - f(\hat{\epsilon}_k + eV)] d\hat{\epsilon}_k \quad 2-61$$

where the $T^2 D^2$ term again can be taken outside the integral. This is the first point at which the rigorous physically based theory coincides with the phenomenological approach most often used.

By noting that:-

$$f(\hat{\epsilon}_k) - f(\hat{\epsilon}_k + eV) = \begin{cases} 1 & \text{for } 0 < E < eV \\ 0 & \text{E} > eV \text{ or } E < 0 \end{cases}$$

equation 2-61 becomes eV

$$I_{NS} \propto T^2 D_1(\epsilon_f) D_r(\epsilon_f) \int_0^{eV} \frac{|E|}{(E^2 - \Delta^2)^{1/2}} dE$$

where $dE = d\hat{\epsilon}$ since at $T = 0$, Δ is constant. Finally therefore

$$I_{NS} \propto T^2 D_1(\epsilon_f) D_r(\epsilon_f) [(eV)^2 - \Delta^2]^{1/2} \quad 2-62$$

For the case $T \neq 0$ the integral is complicated but has been solved.

If we now differentiate this expression for I_{NS} with respect to V and divide the result by the derivative of I_{NN} with respect to V , we find that the ratio of these dynamic conductances is:-

$$\frac{\sigma_{NS}}{\sigma_{NN}} = \frac{eV}{[(eV)^2 - \Delta^2]^{1/2}} \quad 2-63$$

This expression is precisely the normalised density of states for a superconductor as can be seen from the expression 2-37 derived earlier.

We have thus proved that by measuring the normalised dynamic conductance of an N - S tunnel junction we are in fact measuring the electronic quasiparticle density of states of the superconductor. Because of this, fundamental properties such as T_c and $\Delta(0)$ are directly obtainable.

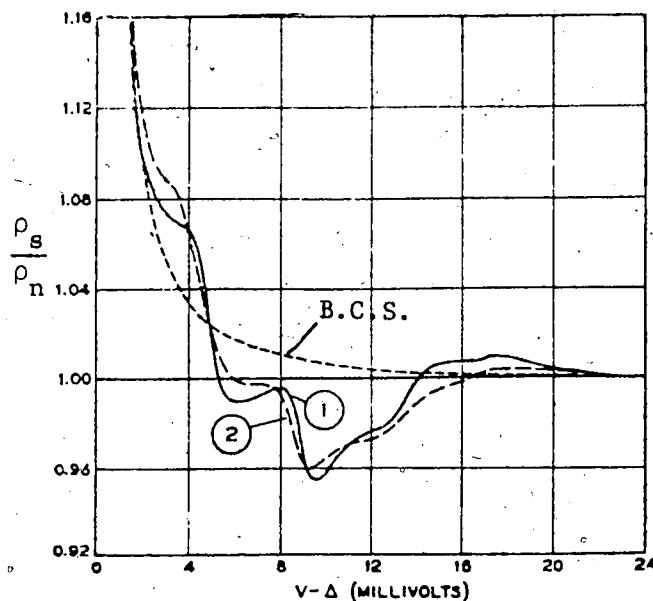
7. Strong Coupling Theory

Whilst the weak coupling theory describes most superconductors extremely well and all superconductors to first order there are some which deviate considerably from its predictions. Mercury and lead are two such examples. Experimental evidence shows the

condensation energy for lead to be less than that predicted using the B.C.S. model and outside the limits of experimental error.

The "universal" constant of equation 2-47 relating the gap to transition temperature for lead was found to be 4.47 instead of 3.53.

Yet another striking difference is exhibited by these superconductors in the density of states as observed by tunnelling in that there is considerable departure from the smooth function expected on the basis of equation 2-37. This was first observed in the tunnelling experiments of Giaver et. al. (1962) and Rowell et. al. (1963) and is illustrated below for the case of lead which shows the B.C.S. prediction and the experimentally observed tunnelling density of states of Rowell et. al. (curve (2)) taken from R.D. Parks.



It became clear in the light of such experimental evidence that the existing theory of superconductivity must be modified to explain these differences in behaviour in a class of metals which

have become known as strong-coupling superconductors. The first attempt was to try and extend the weak coupling theory by removing the assumption on the product DV . This was done by D.J. Thouless (1960) who found that even in the unphysical limit of $DV \rightarrow \infty$ the ratio $2\Delta(0)/k_B T_c \rightarrow 4.00$ and although this was a step in the right direction it could not fully account for the observed deviations. The next step was taken by Swihart (1962) who replaced the simple B.C.S. constant potential with a more realistic one. This refinement met with some success but still could not account for the structure in the density of states curve. The correct formalism was finally arrived at through the realisation that the electron-electron interaction, which according to the B.C.S. model was instantaneous, was in fact retarded. This can be understood since the phonons involved with the pairing of electrons move with a phase velocity very much less than the Fermi velocity of the electrons and thus there is a time lag before the second electron "feels" the existence (or is influenced by) the first. In addition to retardation effects, lifetime effects were proposed associated with the damping of quasiparticle excitations. This approach was adopted by Migdal (1958), Nambu and Eliashberg (1960) and Eliashberg (1962) using field theoretic Greens functions (since potentials that are retarded in time cannot be treated with Hamiltonian dynamics).

The results of this analysis are presented below:-

$$\phi(\omega) = \int_0^{\omega_c} d\omega' \operatorname{Re} \left[\frac{\Delta'}{(\omega'^2 - \Delta'^2)^{1/2}} \right] [K_+(\omega, \omega') - N(0)U_c] \quad 2-64$$

$$\omega[1 - Z(\omega)] = \int_0^{\omega_c} d\omega' \operatorname{Re} \left[\frac{\omega'}{(\omega'^2 - \Delta'^2)^{1/2}} \right] K_-(\omega', \omega) \quad 2-65$$

where

$$K_{\pm} = \sum_{\lambda} \int_0^{\omega} d\nu \alpha_{\lambda}^2(\nu) f_{\lambda}(\nu) [(\omega' + \omega + \nu + i0^+)^{-1} \pm (\omega' - \omega + \nu - i0^+)^{-1}]$$

Equations 2-64 and 2-65 are referred to as the strong-coupling-gap equations. A third relationship is introduced in the form:-

$$\Delta(\omega) = \phi(\omega)/Z(\omega) \quad 2-66$$

ω_c represents a cut off energy usually taken to be $\approx 10\omega_D$, U_c is the Coulomb pseudopotential characterising the short range repulsive force between electrons and $Z(\omega)$ is a renormalisation function given by:-

$$\varepsilon(k, \omega) = \varepsilon/Z(\omega)$$

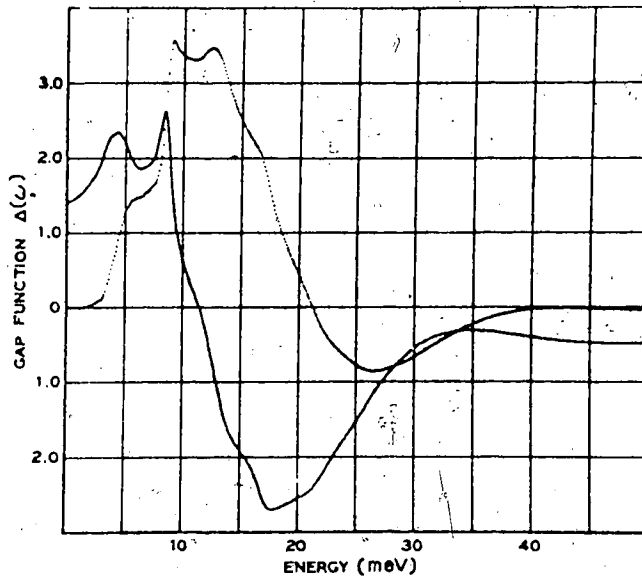
where ε represents a single particle energy (Bloch state).

We can see that these coupled equations for Δ are complex as is Δ itself in the general case. Clearly Δ is also a function of energy. It may be written in the form

$$\Delta(\omega) = \Delta_1(\omega) + i\Delta_2(\omega) \quad 2-67$$

The $\alpha_{\lambda}^2(\nu)$ represents a coupling function associated with the electron phonon interaction whilst the function $f_{\lambda}(\nu)$ takes account of the specific nature of the phonon spectrum of the particular material under investigation. Thus we see some marked differences in this formalism from the B.C.S. approach although in the weak coupling limit the quantity $\Delta(\omega) \rightarrow \Delta(0)$ enabling us to identify $\Delta(\omega)$ with the superconducting energy gap still. To obtain $\Delta(\omega)$ we must first solve the integral equations 2-64 and 2-65 self consistently and then apply equation 2-66. An example of the form of the gap function is shown below for the case of lead due to McMillan and Rowell (1969)

Real (—) and imaginary (...) parts of the computed energy gap function $\Delta(\omega)$ for Pb vs. $\omega - \Delta(0)$.



The gap function assumes a constant value at some given energy which is consistent with the minimum energy necessary for pair creation. The point at which this occurs is known as the gap edge and is the place at (or below) which the gap value is usually measured.

We saw earlier that in the weak coupling approximation of $DV \approx 10^{-1}$ that a universal constant of 3.53 resulted for the ratio $2\Delta(0)/k_B T_c$ and whilst this approximation is not valid for strong coupling superconductors by definition, it is used instead as a guide to the strength of coupling; the higher its value the stronger the coupling is presumed to be. Clearly since both Δ and T_c have the same functional dependence on the product DV , then we would not expect there to be any deviation in $2\Delta(0)/k_B T_c$ as a result of increasing coupling strength DV . Lead for example, however exhibits a value of 4.47 for $2\Delta(0)/k_B T_c$. This is thought to be due to

inelastic phonon processes causing damping of quasiparticle states and although this would reduce both $\Delta(0)$ and T_c , the effect on T_c would be greater since there would be more thermal phonons present at T_c (as T_c for lead is high). Such a calculation has been carried out for lead on this basis by Wada (1964) with a prediction of $2\Delta(0)/k_B T_c = 5.2$

An expression for $2\Delta(0)/k_B T_c$ has been derived for strong coupling superconductors by Geilikman and Kresin (1965) given by

$$\frac{2\Delta(0)}{k_B T_c} = 3.52 \left[1 + \frac{5.3 T_c^2}{\omega_0^2} \left(\frac{\omega_0}{T} \right) \right] \quad 2-68$$

where ω_0 is the limiting frequency of longitudinal phonons.

Another indicator as to the strength of the coupling is the nature of the quantity $DV = \lambda$ which is regarded as the electron-phonon coupling strength. For weak coupling this was assumed to be of the order 10^{-1} whilst for the system under consideration here it is of the order unity. The quantity λ is given by

$$\lambda = 2 \int_0^{\infty} \frac{d\omega \alpha^2(\omega) F(\omega)}{\omega} \quad 2-69$$

$$\text{and } 1 + \lambda = \frac{m^*}{m} \quad 2-70$$

where m^* is the effective mass of the electron. A further indicator is associated with α , the coupling function appearing in the gap equation, which is usually expressed as an average given by:-

$$\langle \alpha^2 \rangle = \frac{\int_0^{\infty} \alpha^2(\omega) F(\omega) d\omega}{\int_0^{\infty} F(\omega) d\omega} \quad 2-71$$

Increases in the values of λ , $\langle \alpha^2 \rangle$ and $2\Delta(0)/k_B T_c$ are associated with increases in the coupling strength. In the experiments that were conducted Δ and T_c were directly measured whilst λ and $\langle \alpha^2 \rangle$

(together with other microscopic parameters such as μ^* the Coulomb pseudopotential) were obtained indirectly by a process of inversion of the strong coupling gap equations. The inversion program will be discussed in more detail in a later chapter.

An expression for the transition temperature of strong-coupling superconductors has been proposed by McMillan (1968) in the form

$$T_c = \frac{\langle \omega \rangle}{1.20} \exp \left[- \frac{1.04 (1 + \lambda)}{\lambda - \mu^*(1 + .62\lambda)} \right] \quad 2-72$$

If we differentiate this expression we get (assuming $d\mu^*/dp = 0$):

$$\frac{d \ln T_c}{dp} = \frac{d \ln \langle \omega \rangle}{dp} + 1.04 \left[\frac{1 + .38\mu^*}{(\lambda - \mu^* - .62\lambda\mu^*)^2} \right] \frac{d\lambda}{dp} \quad 2-73$$

Those quantities on the right hand side of this equation are derivable from the inversion process whilst T_c is directly measurable and we are thus able to check the overall "quality of the inversion" technique against experiments.

Scalapino, Schrieffer and Wilkins (1963, 1966) applied the principles of strong-coupling theory to the calculation of the normal metal superconductor tunnelling current and showed that the expression 2-63 still holds in the following form:-

$$\frac{\sigma_{NS}}{\sigma_{NN}} = \frac{\text{Re} |eV|}{\left[(eV)^2 - \Delta^2(\omega) \right]^{1/2}} \left[\frac{D(E)}{D(\epsilon_f)} \right] \quad 2-74$$

Using a very simple form for the phonon spectrum of lead which they approximated by two Lorentzians situated at ≈ 4.4 meV and 8.5 meV, Schrieffer, Scalapino and Wilkins (1963) calculated the gap function and then the normalised conductivity for the NS case at non zero temperature. These results are shown in the diagram on page 30 (fig. (1)) in which we can see that there is excellent qualitative agreement with the

experimental observations of Rowell et. al. (1969).

8. Observation of Phonon Structure by Tunnelling

We have now seen that inclusion of the form of the phonon spectrum leads to structure in the normalised density of states curve obtained by tunnelling (from the results of Rowell et. al. for example). That this is plausible can be shown by examining the form taken by the expression for the normalised conductivity $\sigma = \sigma_{NS} / \sigma_{NN}$ in the light of the strong-coupling theory

$$\sigma = \frac{\text{Re}|\omega|}{(\omega^2 - \Delta^2(\omega))^{1/2}} \quad \text{where } \omega = eV \quad 2-75$$

expanding by the binomial theorem and using equation 2-67 we get

$$\sigma = 1 + \frac{\Delta_1^2(\omega) - \Delta_2^2(\omega)}{2\omega^2} + \dots \quad 2-76$$

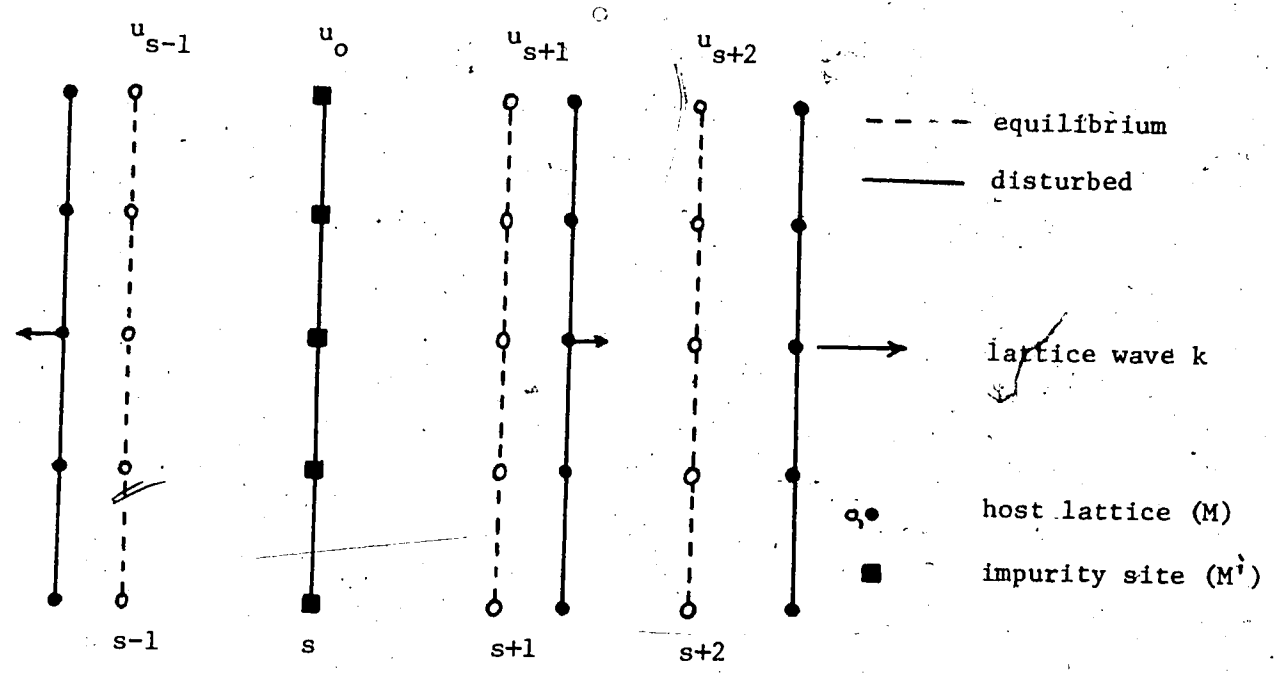
Since $\Delta(\omega)$ clearly depends on $F(\omega)$ (inherent in the strong-coupling equations) then the normalised conductivity that we monitor in electron tunnelling experiments must also be influenced by the phonon spectrum of the metal. Quasiparticles whose energies coincide with the predominant phonon modes of a given metal have a high probability of phonon emission with subsequent decay to the peaked region in the density of states (at the gap edge). We therefore observe larger changes in the conductivity at these points. Scalapino and Anderson (1963) have shown that such resonances in $F(\omega)$ give rise to points of inflection in the density of states. This can also be seen by careful study of the effects of Δ_1 and Δ_2 on using 2-76. We are therefore provided with a powerful tool for

resolving principle phonon peaks of a metal since differentiation of the conductivity curve will give rise to maxima and minima at these inflection points.)

For the lead-indium system under investigation the principle phonon peaks are those of the lead lattice but with the addition of an extra peak at the high energy end of the spectrum. This extra peak is associated with inclusion of a small amount of indium impurity in the host lattice. Justification for its existence is the subject of the next section.

9. The Localised Mode

To verify the existence of a localised mode of vibration in a solid which contains a light substitutional impurity let us consider the simple one dimensional case below:-



We now consider the dynamical problem arising when one row of atoms M is replaced by the light impurity M' as a longitudinal wave passes through the crystal. Assuming only nearest neighbour interactions and further that the force constant c for these interactions is constant (unchanged by the presence of M') we have for the equations of motion of the s plane of atoms

$$M' \frac{d^2 u_0}{dt^2} = c(u_1 + u_{-1} - 2u_0) \quad 2-77$$

and for the $(s + 1)$ plane

$$M \frac{d^2 u_1}{dt^2} = c(u_2 + u_0 - 2u_1) \quad 2-78$$

where the u represent displacements of the planes of atoms from their undisturbed positions. Using a trial solution of the form

$$u_s = u_0 (-1)^s e^{-i\omega t} e^{-|s|\alpha} \quad 2-79$$

a self consistent solution is obtained for 2-77 and 2-78 if

$$e^\alpha = \frac{2M - M'}{M'}$$

hence

$$\omega^2 = \frac{4c}{M} \left(\frac{M^2}{2MM' - M'^2} \right) \quad 2-80$$

Similar treatment of the case when $M = M'$ (no impurity) yields, for

a travelling wave solution of the form $u_{s+p} = u(0)e^{i(s+p)ka - i\omega t}$

$$\omega^2 = \frac{4c}{M} \sin^2 ka$$

This has a maximum value $\omega^2 = 4c/M$ thus substituting in 2-80 we get

$$\omega_{\text{local}}^2 = \omega_{\text{max}}^2 \frac{M^2}{2MM' - M'^2} \quad 2-81$$

as the predicted frequency for the local mode of vibration.

For the case at hand of indium in lead we can treat the indium as such a light impurity. Indium (face centred tetragonal) alloys with lead (face centred cubic) to concentrations of up to 65 atomic % In to give a substitutional f.c.c. structure. To obtain an approximate value for ω_{local} we put $M = 207.2$, $M' = 114.8$ (the atomic weights of Pb and In respectively) and take ω_{max} to be the cut off in the Debeye spectrum of lead and we get that

$$E_{\text{local}} \approx 9.83 \text{ meV}$$

This prediction is in fact in excellent agreement with that observed as will be seen. Whilst it is realised that such agreement is fortuitous in the light of the assumptions made it is noteworthy that the more complex Greens function approach using Dysons equation yields an expression identical to that of equation 2-81.

CHAPTER III

EXPERIMENTAL APPARATUS

1. The Cryostat

A conventional double glass dewar system was used to cool the main body of the cryostat, a cross section of which is shown in figure 1. The original design and construction of the cryostat was carried out by Franck and Keeler (1968) for their work on pure lead and was used, after extensive modification, for this work. The cryostat basically consisted of three self contained systems.

The first of these was a beryllium-copper chamber (which will be referred to hereafter as the bomb) in which the tunnel junctions to be studied were actually mounted. Commercially supplied high pressure capillary tubing (Harwood Eng. Co. 3M series) was used to connect the bomb to a gas compressor.

The second system consisted of a small copper chamber (~150 ml) attached to the lower end of the bomb by a large copper securing nut and washer. Quick connection of this chamber to the needle valve and a roughing pump were made using swagelock couplings (not shown in diagram). By first admitting liquid helium into this chamber and subsequently lowering its vapour pressure by pumping, temperatures in the region of 1K → 2K could be attained. An indication that such temperatures could be realised can be seen in figure 2 which shows a double gap in a tunnel characteristic obtained from a lead-insulator-aluminium junction. The presence of this double gap is

FIGURE 1

CRYOSTAT

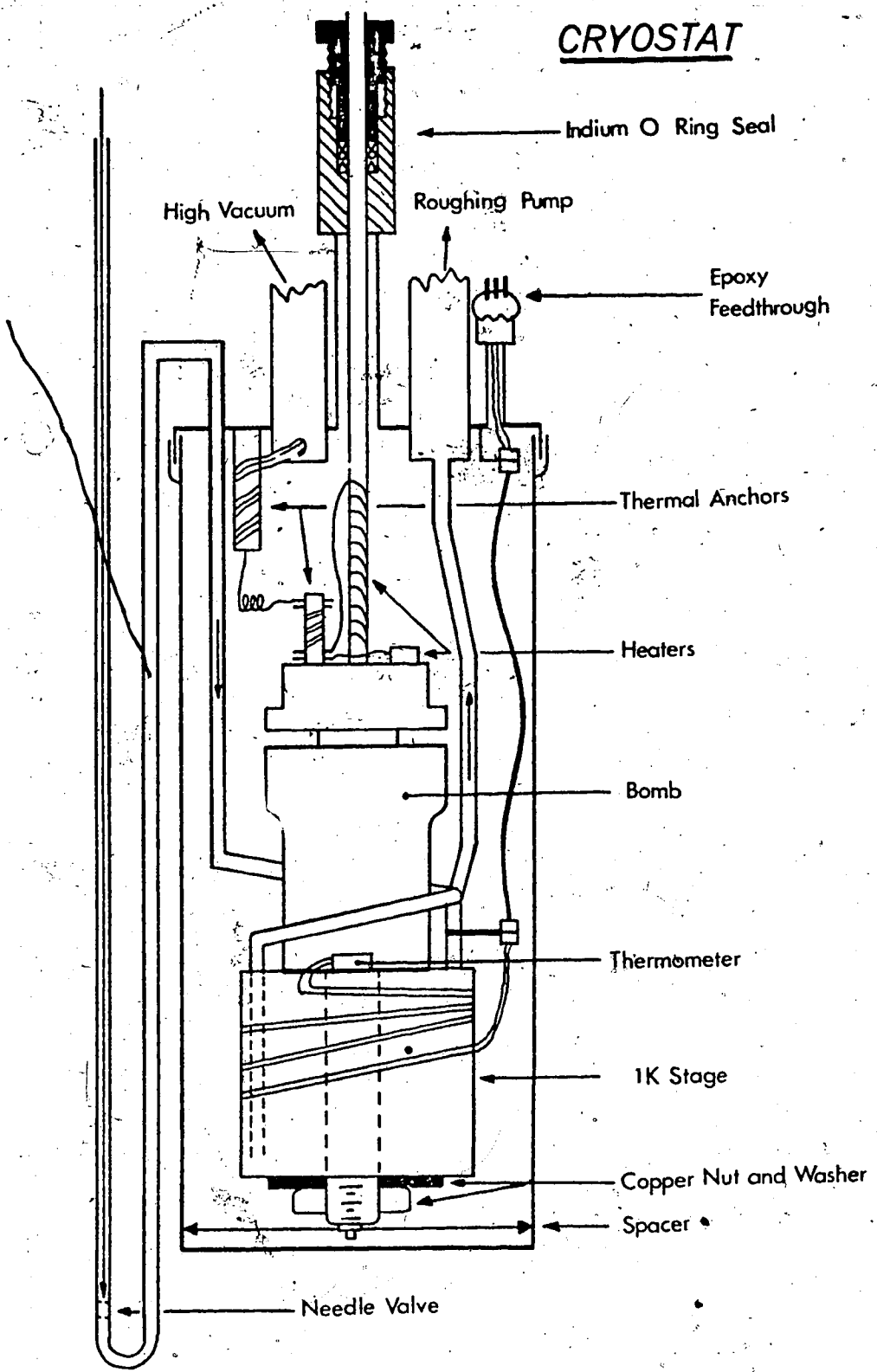
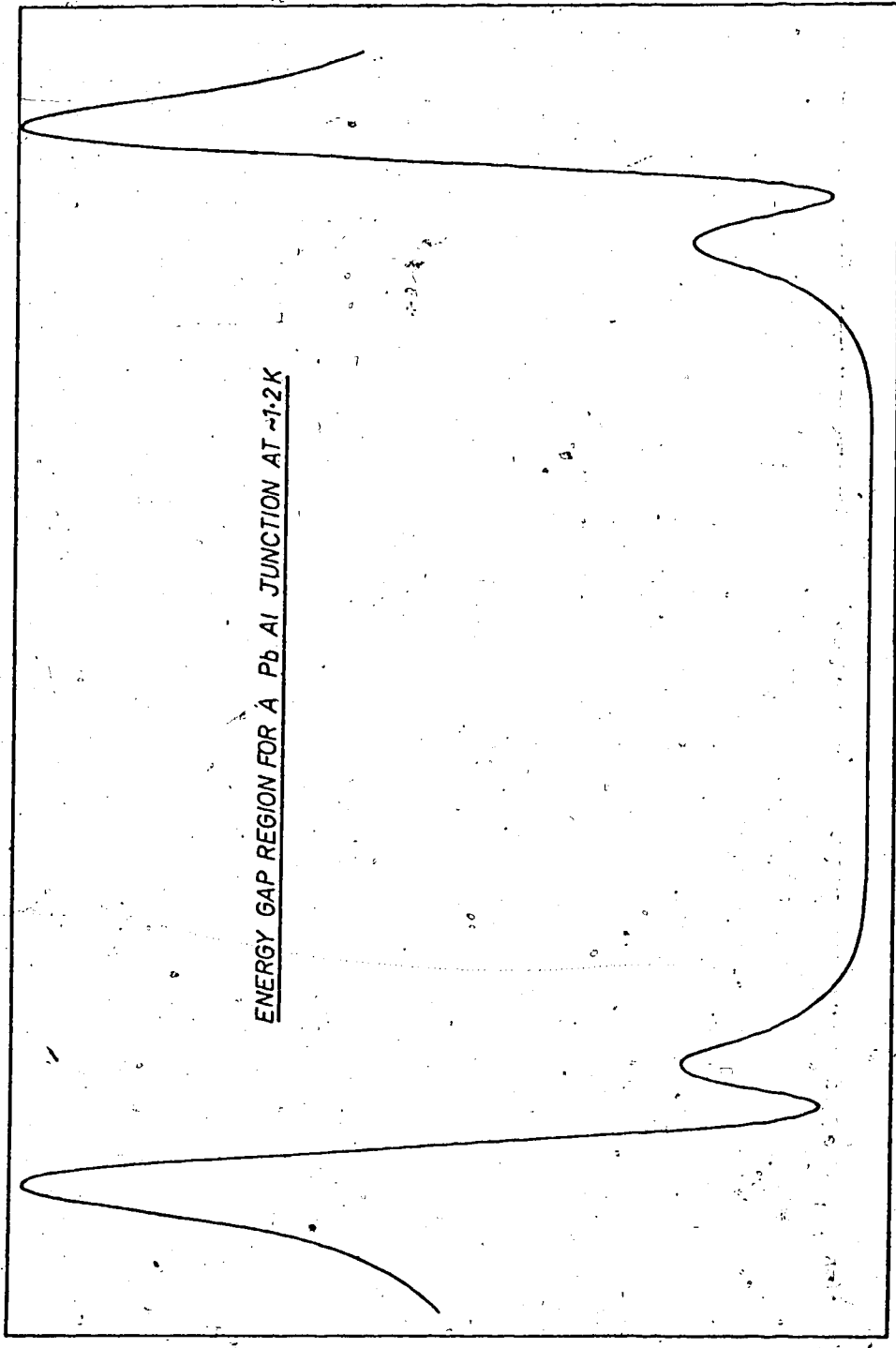


FIGURE 2



attributed to the onset of superconductivity in the aluminium film ($T_c = 1.2K$) and although it is appreciated that thin film effects can cause a rise in T_c to perhaps 2K, this is not thought to be the case here since a temp 2K was confirmed by the thermometry. To obtain the excellent thermomechanical contact necessary for such low temperatures the lower surface of the bomb was carefully lapped to the upper surface of the chamber using a series of Exolon Al_2O_3 lapping compounds and smearing the mated surfaces with a suspension of copper powder in Apiezon N type vacuum grease.

The third self contained system took the form of a large copper can (main vacuum can) enclosing the other two systems and connected to a high vacuum oil diffusion pump. Except when using exchange gas, the pressure inside this can was maintained in the range 10^{-6} torr \rightarrow 10^{-7} torr and provided therefore the necessary thermal isolation of the bomb from the cryogenic fluid in which it was situated.

An indium O ring seal was used to retain the high vacuum at the exit point of the high pressure capillary from this can. This seal was located several inches above the top of the can to provide an extra degree of thermal isolation for the pressure tube and thus reduce the possibility of blockage caused by cold spots.

In order to further minimise the occurrence of blockage, heaters were placed at strategic points including a manganin resistance wire inside the actual pressure tube and running its entire length.

Temperature regulation was also effected in part by these heaters.

Relocation of the needle valve from the can top to its present

position permitted the use of the very simple design shown which was not only leak tight but since it was always totally immersed in the liquid helium, was not susceptible to icing up.

Wires for the heater circuits were admitted to the can through the high vacuum tube (via a room temperature epoxy feedthrough) and thermally anchored by winding several inches of their length on a copper post and securing them tightly with varnish. Two such thermal anchors were employed, one at 4K situated at the can top and the other at ~2K and located at the bomb top. The 2K anchor was constructed in such a way as to be removable in the event of failure of the main wiring (to be described).

After passing through the liquid helium bath, the thermometer leads were led into the high vacuum can via an epoxy feedthrough of the type described by Anderson (1968). From here they were then connected to the 1K pumping stage using a jumper cable wired to Amphenol miniplugs (for quick connection) at which point they were firmly anchored, again using varnish.

The cryostat was used over a temperature range of from 1K → 40K. That such elevated temperatures were necessary can be appreciated from the phase diagram (figure 3) in which it can be seen for example that in order to form a solid at 3.5 kbar temperatures ≥ 35 K are required.

2. The Bomb

Figure 4 shows a cross-sectional view of the bomb and low temperature pumping stage. The bomb itself was machined from an alloy

FIGURE 3

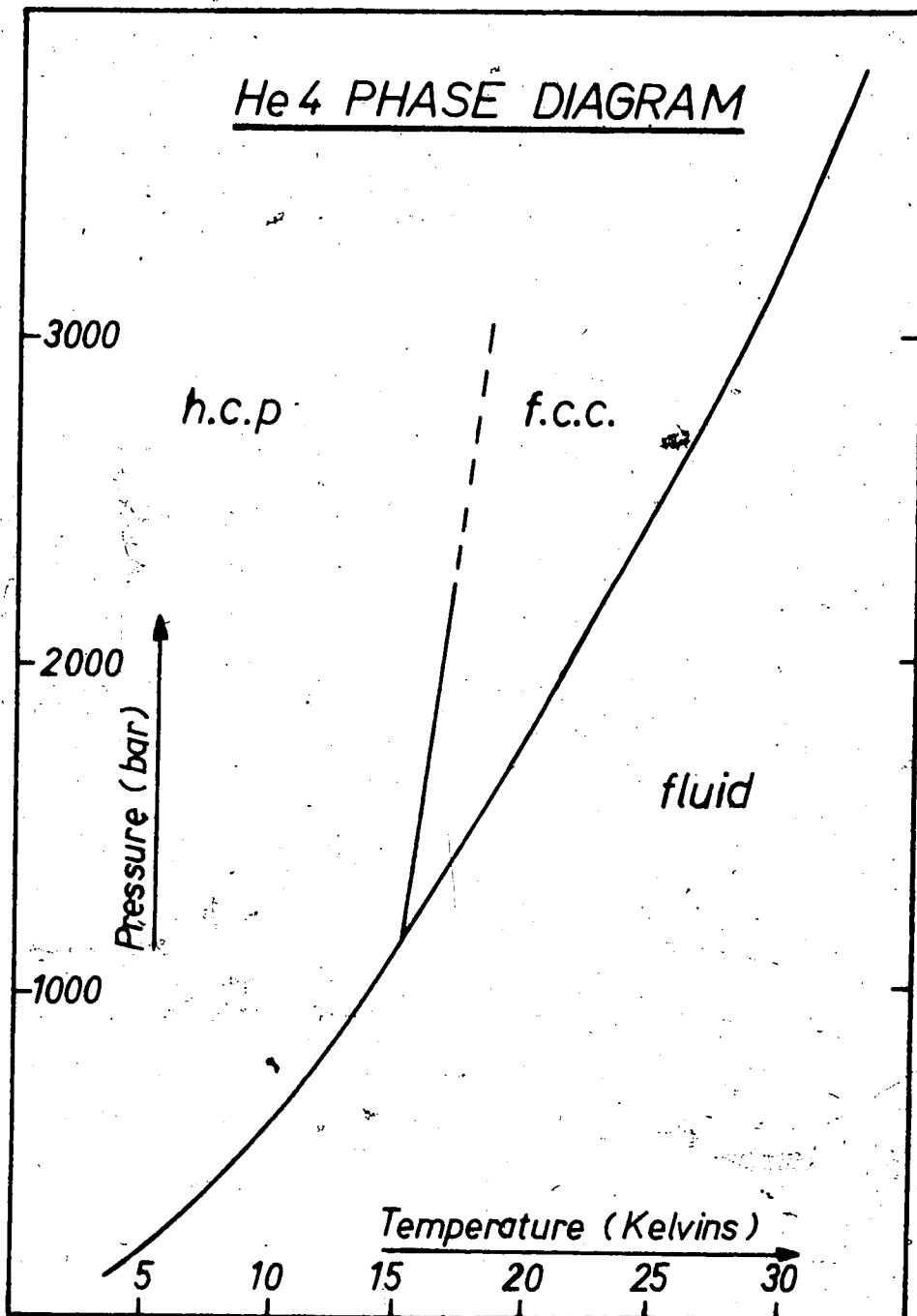
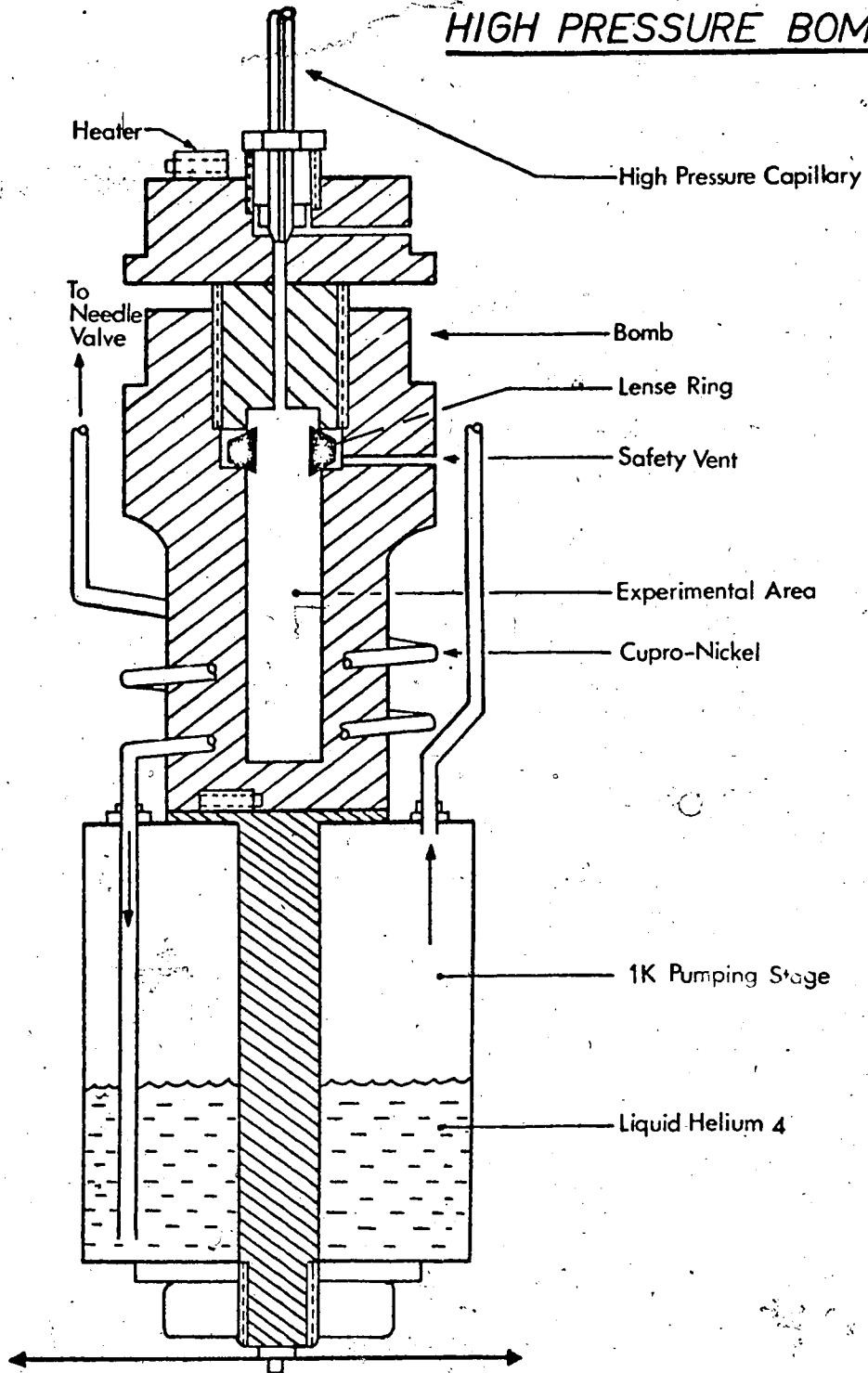


FIGURE 4

HIGH PRESSURE BOMB



containing approximately 98% copper and 2% beryllium (with traces of Co and Ni) which after heat treatment had a tensile strength of ~200,000 p.s.i. The advantages of this alloy are that it exhibits good thermal conductivity and has a strength comparable to stainless steel without embrittling at low temperature.

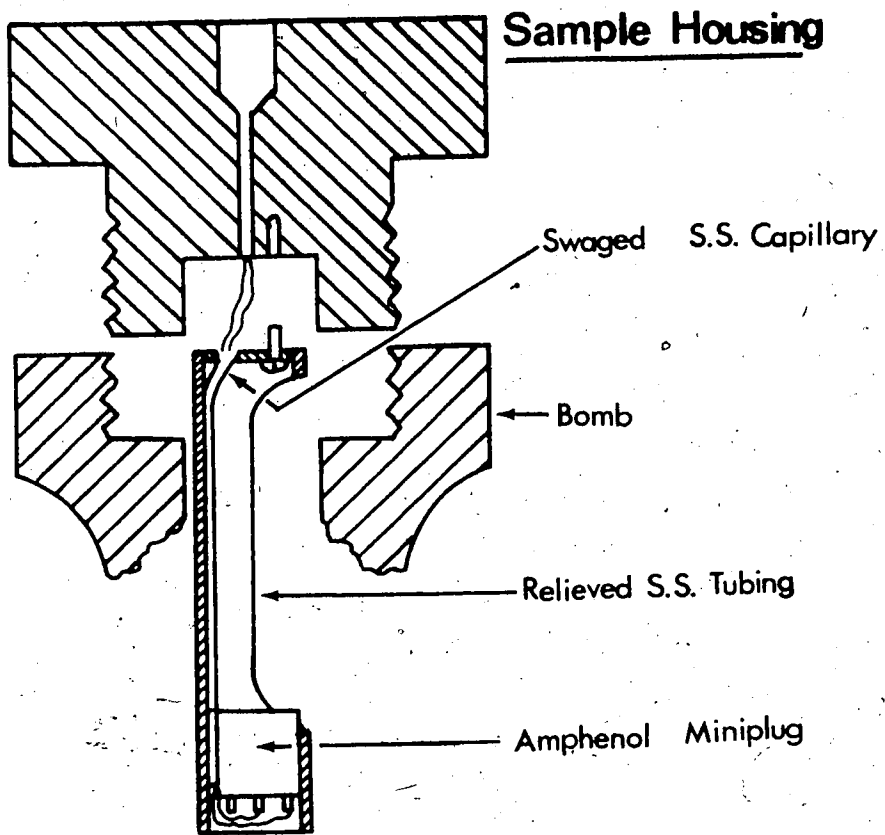
The gas tight seal between the two halves of the bomb was achieved by compressing a specially designed stainless steel ring (lense ring) whose edges had been bevelled at 37° . This particular method provides a self tightening seal since any increase in internal pressure serves to further force the ring onto the sealing edges of the bomb. The core of the bomb was machined to $\frac{1}{2}$ " dia. and to a depth of $\sim 2\frac{1}{2}$ " to accommodate the sample housing.

3 Sample Housing and Holder

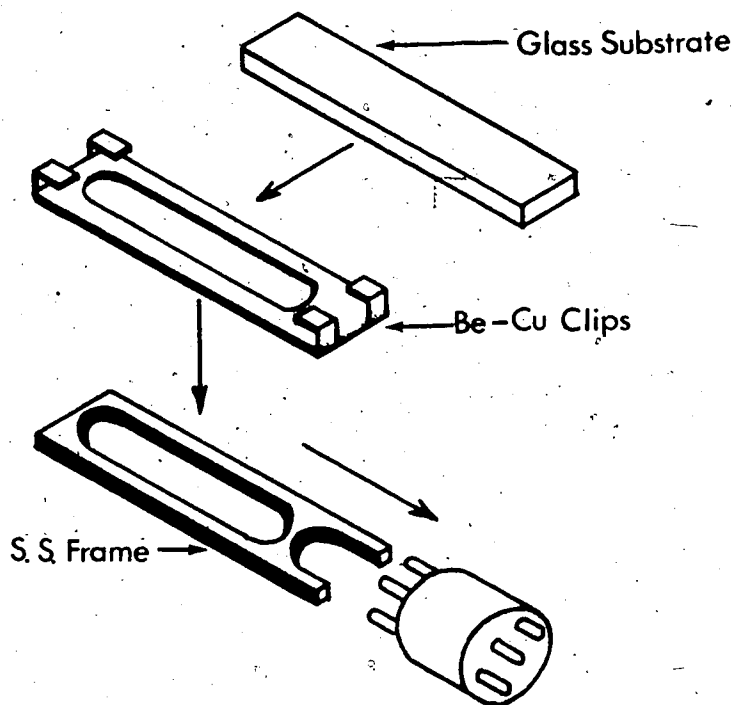
In order to maximise the useable space in the bomb's experimental area a special housing was designed and constructed and is shown in figure 5 together with the sample holder.

The housing consisted of a thin wall stainless steel tube (whose diameter was chosen to be a close fit in the bomb) which had been milled as shown. A thin capillary tube was then swaged slightly at each end and silver soldered to the back of this tube to allow passage of the wires. An Amphenol miniplug was next turned to size, relieved so as to accommodate the capillary and then epoxied into position as illustrated. Having attached a lid to the top end, this device was then secured in place in the bomb top. The use of this housing

FIGURE 5



Sample Holder



allowed the passage of the wires to the bottom end of the plug where they were secured in such a fashion as to be completely safeguarded against breakage.

The sample holder was constructed by first fabricating the base from stainless steel and silver soldering to this the beryllium copper clip arrangement which holds the glass substrate (on which the tunnel junctions are formed). Beryllium copper was chosen for the clips since cold working of stainless steel leads to breakage in this case. This arrangement was then soldered to a compatible plug. The two greatest advantages of this set-up were that it was very fast to mount a specimen whilst eliminating completely the handling of the specimen itself.

4. High Pressure Production and Measurement

High pressure production was achieved using a Harwood Eng. Co. compressor specially adapted for use with gaseous helium four. From an initial supply at 800-1000 p.s.i. the gas was pumped in three successive stages to the 3.5 kilobar range used for these measurements. Isolation of the experimental chamber from the final compressor stage was effected by a needle valve.

Three methods of pressure measurement were employed namely a Heise Bourdon gauge (0-100,000 p.s.i.), a manganin gauge and the tunnel junctions themselves. The manganin gauge supplied with the compressor monitored the pressure dependent resistance of a manganin wire using a Wheatstone bridge circuit and was supposedly accurate

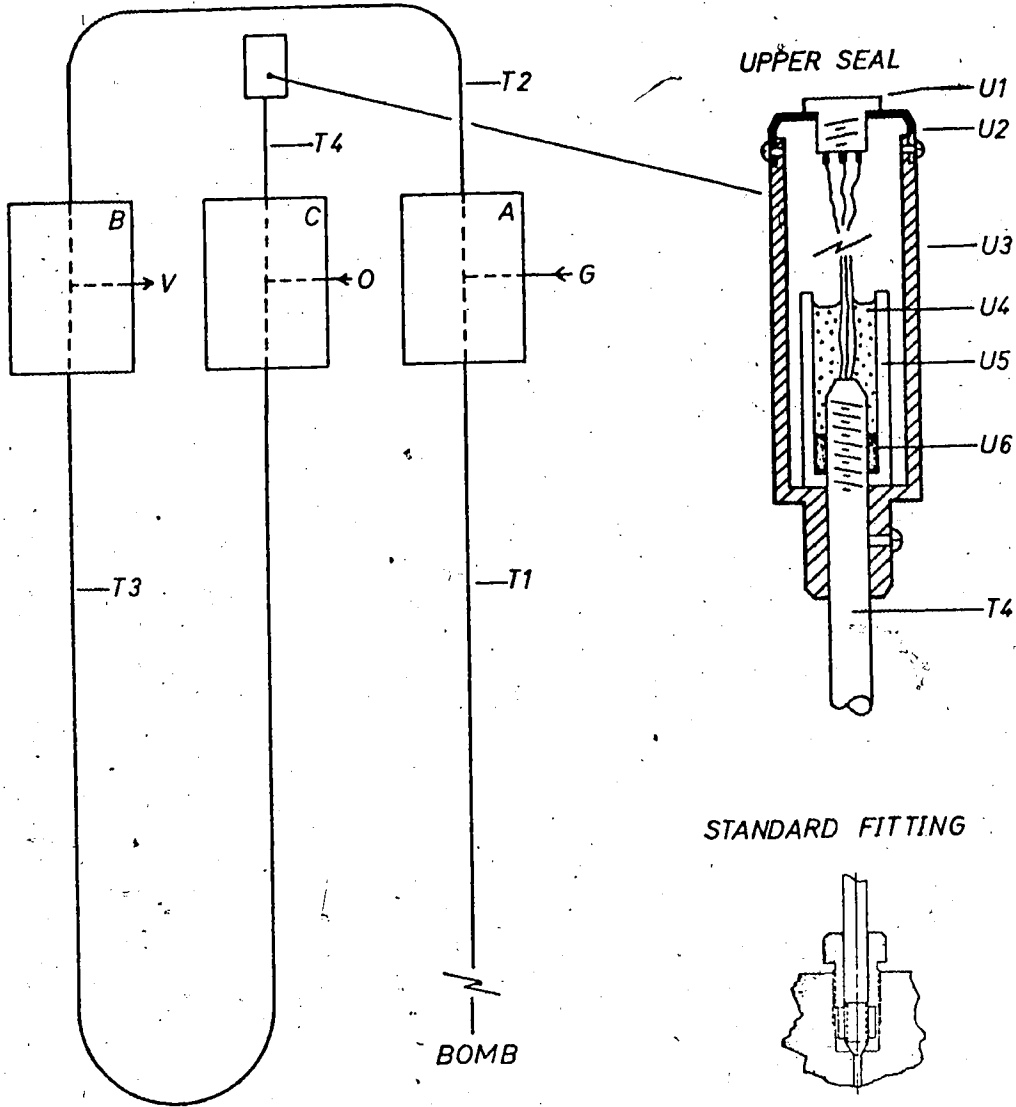
to 1%. This gauge and the Heise Bourdon gauge were used to calibrate the tunnel junction by recording its zero bias resistance as a function of pressure. The final frozen in pressure was always determined using the junction itself since the two other methods would then only monitor external pressure. This method is to be discussed in more detail in a later chapter. Experiment showed that the temperature dependent resistance change of a sample was $<.5\%$ for a ΔT of 70K and thus no correction to pressures was applied in this regard.

5. The High Pressure Electrical Feedthrough

In conducting experiments at high pressures using gaseous helium as the pressure transmitter one is faced with the problem of introducing electrical wires into the experimental chamber without loss of pressure. To overcome this, a seal was constructed based on the frozen oil method employed by Dugdale and Hulbert (1957) and is illustrated in figure 6. An oil-epoxy feedthrough which incorporates this principle has been described by Gorn et. al. (1965), in which heavy emphasis is placed on the role of the epoxy which separates the gas-oil interface. This particular seal was found to be extremely difficult to construct and its failure rate in service found to be high, both of these drawbacks being attributed to the presence of the epoxy. Furthermore a close examination of the defunct feedthroughs revealed that the epoxy had in fact not penetrated the pressure tube to any appreciable extent. This latter problem was due in part to the fact that in the experiments described herein, 6-9 wires were necessary

FIGURE 6

HIGH PRESSURE FEEDTHROUGH



thus providing a major constriction in the pressure tubing.

To this end, a feedthrough was devised for use with large numbers of wires which did not employ the use of epoxy filled tubes. This feedthrough is in comparison very easy to construct and re-fillable as well as incorporating a plug designed to protect wires from accidental damage.

Subject to a specifically ordered filling procedure which prevents contamination of the experimental chamber, the feedthrough illustrated not only survived the test of time but vented itself of oil when the liquid nitrogen level fell; again without contamination of the experimental chamber.

In order to construct the particular seal shown, approximately twelve feet of 3/16" Q.D., .0025" bore stainless steel pressure tubing (Harwood 3M series) was first coned and threaded (for use with the standard fitting shown) and cut to the desired lengths for the tubes T1, T2, and T3. These tubes were then laid out on a long clean surface together with the junction blocks and fittings in a development which would ultimately lead to the final form shown. Having passed the required number of wires through the system and allowing an excess at each end, the fittings were carefully tightened and the feedthrough bent to shape.

The principle involved in retaining the gas pressure with such an arrangement would be to fill the tube T3 with oil by admitting it through O in block C and then immersing T3 in liquid nitrogen. In order to prevent the preferential leakage of oil at the top of block

C during filling it was necessary to block T4. To this end a reusable device (upper seal in illustration) was constructed which not only blocked T4 but accommodated a plug so that the wiring could be accessed without exposure to possible breakage. Since T4 was never called upon to more than two or three thousand p.s.i. oil pressure, a standard - but still standard - pressure tube was used of 1/4" and a bore of 1/16" (Harwood 4L series).

To assemble the upper seal, the main body of machined brass (U3) and the stainless steel cup (U5) were first slid onto the tube followed by the standard threaded collar (U6). The stainless steel cup was held in position and filled with Stycast 2850 G.T. epoxy which was allowed to cure. Some of this epoxy is also expected to enter T4 and, although favourable, is not essential to the operation of the seal. The protruding wires were then attached to an Amphenol miniplug (U1) housed in the machined brass cap (U2). Finally the main body was raised into position and locked onto the tube and the cap secured.

To fill the seal, very low pressure helium gas was pumped into block A through G and allowed to leak slowly from the vent V. Simultaneously, oil was pumped at low pressure into block C through O and thus through tube T3 to block B and also allowed to leak from V. It was felt that the steady stream of gas in T2 would prevent the slight possibility of oil leaking into this tube. Having established a continuous bubble free flow of oil from the vent, the tube T3 was immersed in liquid nitrogen. When the oil ceased to

flow, the oil pressure was reduced to zero and the vent valve V tightened whereupon the system pressure was observed to rise as expected. The bomb remained in position throughout the filling process. The system described is now ready for use and will remain so if the nitrogen level is maintained.

When not in active use (or when deliberately venting the oil seal) the bomb was kept in place containing a few hundred p.s.i. of gas pressure while the oil supply line O remained vented. This practice ensured that if the nitrogen trap was left untended the melted oil would be ejected from O and eliminate any possibility of contamination of T1 via T2. Should this occur it would be necessary to recharge the seal by repeating the above procedure.

6. Vacuum Deposition

The tunnel junctions were formed by evaporation in a customised Norton Research Company 3115 model high vacuum system. Masks were fashioned from stainless steel to give the required film geometry and an enlarged contact area and located in a carousel which allowed up to six different source-mask combinations to be used. The carousel was enclosed in a large glass tube, with quartz glass divisions to prevent mutual contamination of sources and masks.

An arrangement compatible with the sample holder described previously was incorporated in the carousel design in such a way as to allow any desired mask to be raised into contact with the substrate. Since the back of the sample holder had been machined away, it was

possible (with the aid of a prism) to view the film during formation.

7. Temperature Measurement

Temperatures were measured with the aid of a commercially supplied calibrated germanium resistance thermometer (Cryocal), the calibration range being from 1.5K to 40K.

The 1.5K to 2.0K readings were based on the Helium Vapor Pressure Scale of 1958 with an accuracy of 0.003K while the 2.25K to 13K readings are traceable to the National Bureau of Standards Provisional Scale of 1965 (2-20°K) through secondary standards maintained by CryoCal, Inc. with an accuracy of 0.005K from 2K to 5K and 0.01K from 5K to 13K.

The 14K to 40K readings are traceable to the International Practical Temperature Scale of 1968, again through secondary standards maintained by CryoCal, Inc. with an accuracy of 0.01K from 14K to 20K and 0.04K from 22K to 40K.

Resistance values were obtained to better than .1% using potentiometric techniques.

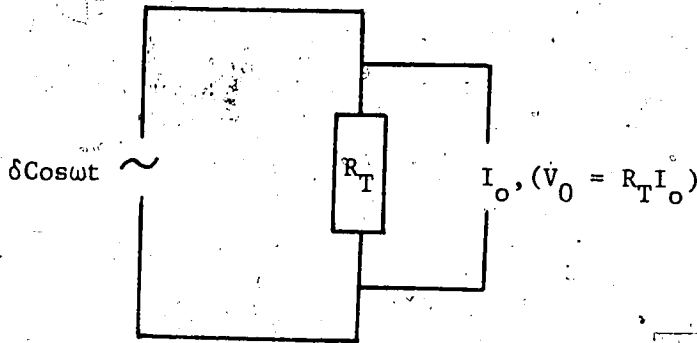
Standard curve fitting procedures were employed for interpolation (and extrapolation where necessary) with excellent reliability.

CHAPTER 4

ELECTRONIC DETECTION TECHNIQUES

1. The Principle of the Measurement

It was shown earlier (Chapter 2) that the quasiparticle density of states in a superconductor was in one to one correspondence with the normalised dynamic conductance σ_{NS}/σ_{NN} as measured, in a normal-superconductor (NS) tunnel junction. Measurements of this quantity were made using standard harmonic detection techniques by applying a small constant a.c. signal across the tunnel junction and monitoring its a.c. response. Considering the idealistically simple circuit shown below



where a constant a.c. signal $\delta \cos \omega t$ (current or voltage) is applied across the sample R_T together with a d.c. bias current I_0 . The signal developed across the sample resistance R_T therefore may be expressed using a Taylor series expansion as:-

$$V(I) = V(I_0 + \delta \cos \omega t) = V(I_0) + \left. \frac{dV}{dI} \right|_{I_0} \delta \cos \omega t + \frac{1}{4} \left. \frac{d^2V}{dI^2} \right|_{I_0} \delta^2 \times (1 + \cos 2\omega t) + \dots \quad 4-1$$

where $\delta \cos \omega t$ here represents a constant a.c. current supply.

If we now let $\delta \cos \omega t$ represent instead a constant voltage supply we obtain in a similar manner:-

$$I(V) = I(V_0 + \delta \cos \omega t) = I(V_0) + \left. \frac{dI}{dV} \right|_{V_0} \delta \cos \omega t + \frac{1}{4} \left. \frac{d^2I}{dV^2} \right|_{V_0} \delta^2 \times (1 + \cos 2\omega t) + \dots \quad 4-2$$

where in both equations 4-1 and 4-2 use has been made of a trigonometric identity. Thus we can see that if we can measure the components of the signal across R_T that are proportional to ω and 2ω we are in fact measuring quantities directly proportional to the dynamic resistance (or conductance) and its derivative. The component proportional to ω is used to yield $\sigma_{NS} / \sigma_{NN}$ whilst the component proportional to 2ω is used to resolve structure in the density of states.

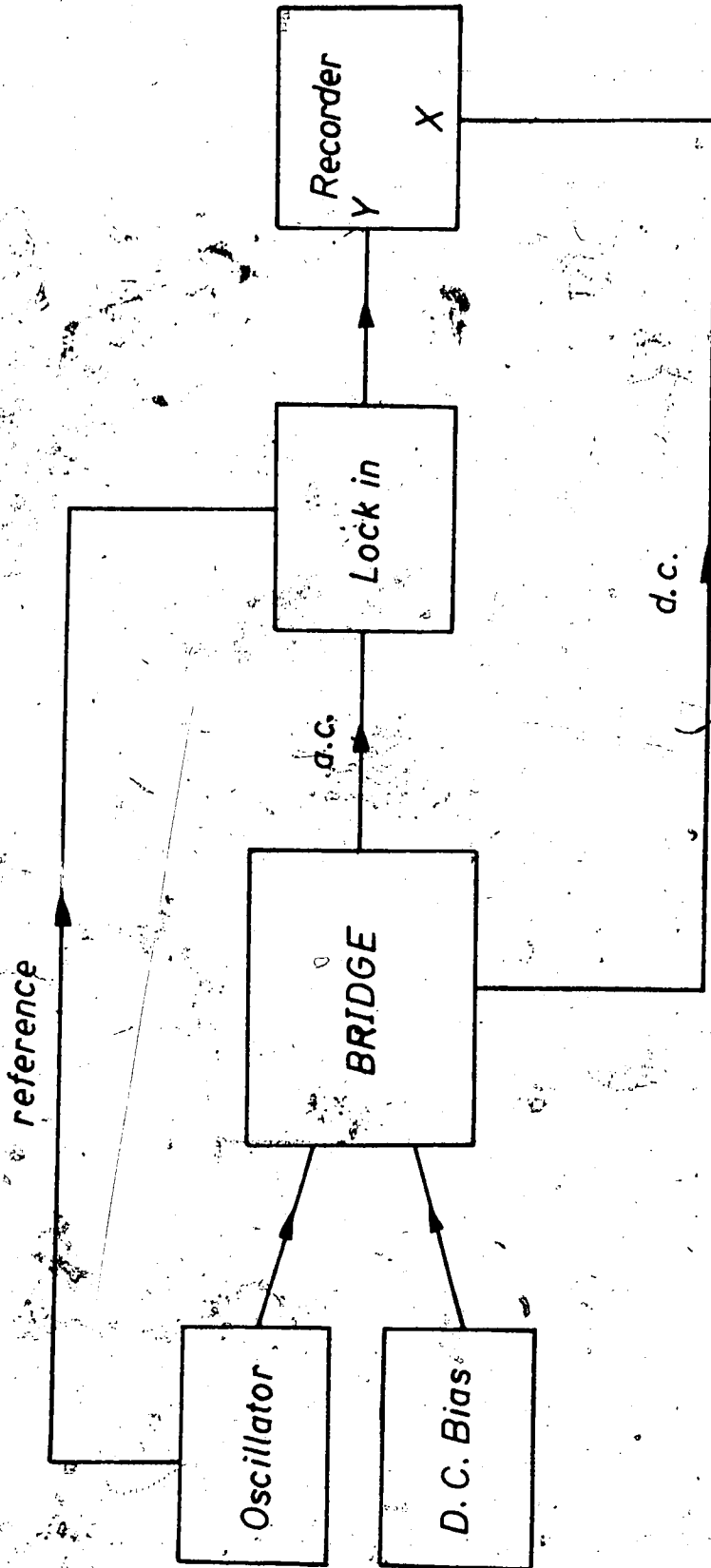
2. Detection of the Harmonics

In order to measure the amplitudes of the components of ω and 2ω , phase sensitive detection techniques were employed using the circuit logic shown in figure 7.

An a.c. signal is applied across the tunnel junction which is incorporated as one arm of a bridge circuit. By so doing we are able to balance out the large component of fundamental and observe only the small non linear changes associated with dV/dI etc. The

FIGURE 7

CIRCUIT LOGIC



response of the tunnel junction is then fed to the input of a phase sensitive lock-in amplifier (P.A.R. HR8) whose phase is set initially to zero and whose band pass is on the source frequency. Simultaneously a reference signal from the same source is fed to the lock-in amplifier and in this way we are able to observe the component proportional to ω . The source of a.c. supply should be as stable in amplitude as possible and, less critically, stable in frequency. Variations in oscillator amplitude are most serious since not only do they manifest themselves directly at the lock in output, but sweep times associated with each curve traced might range up to an hour in duration. Slight drift in frequency is not so serious (depending on the band pass) since the reference supply is derived from the source. The bridge circuit is balanced by minimising the output from the lock-in amplifier (for a specific d.c. bias condition) both resistively and capacitively, in the latter case the phase at the lock-in is shifted by 90° . Having done this (and returned the phase of the detector to zero) unbalancing of the capacitive circuit should cause no appreciable effect on the output of the lock in. Finally while locked onto the resistive component of the sample the d.c. bias is changed slightly causing an unbalanced bridge condition and corresponding output signal from the lock-in. Fine adjustments of the phase and frequency are then made to maximise this output.

The system is thus tuned for maximum response to the first harmonic content. In order to detect the second harmonic component it is only necessary to change the oscillator frequency to $\omega/2$ while

leaving the lock-in tuned to ω .

The output from the lock-in is then fed to a recorder where it is plotted as a function of applied d.c. bias using an X - Y recorder. The desired amplification required is achieved by the combined effect of the variable gains of lock-in and pen recorder.

3. Circuit Design Considerations

Since the tunnelling experiments carried out were in the Fermi surface region it is essential that the measuring technique itself should not interfere with the Fermi surface shape. The temperature dependence of the Fermi surface shape is often alluded to as thermal smearing, an effect which becomes less pronounced as the temperature decreases. At 1K for example the thermal smearing is $\approx 86\mu\text{eV}$ r.m.s. To this end it is essential that the a.c. level (modulation) applied across the tunnel junction by the circuit be as small as possible and less than the thermal smearing at the temperature of the measurements.

In the expansions given by equations 4-1 and 4-2, the component of the first harmonic is already small compared to that of the fundamental but with the further restriction of low applied signal levels and the fact that the tunnel junction response is only weakly non linear, it is necessary to incorporate the tunnel junction in a bridge circuit in which the large fundamental component can be balanced out.

Two such bridge circuits were employed for this purpose one

being a constant current device of the type used by Adler and Jackson (1966) and the other a constant voltage device due to Rogers (1970). These circuits are shown in detail in Figures 8 and 9 respectively, the former showing the support systems which were used for both.

The constant voltage bridge was used for measurements in the immediate energy gap region where the sample resistance approaches ∞ . This avoids the problem of over modulation associated with the constant current bridge and consequent smearing of data. Both bridge circuits allowed four terminal measurements to be made and included large resistors to swamp the normal state resistance of the film electrodes. The detailed circuit for d.c. biasing (sweep) is shown in figure 10.

4. The Constant Current Bridge

The diagram below shows a simplified form of the resistance bridge circuit used in which R_T represents the sample and R_D the bridge balancing components.

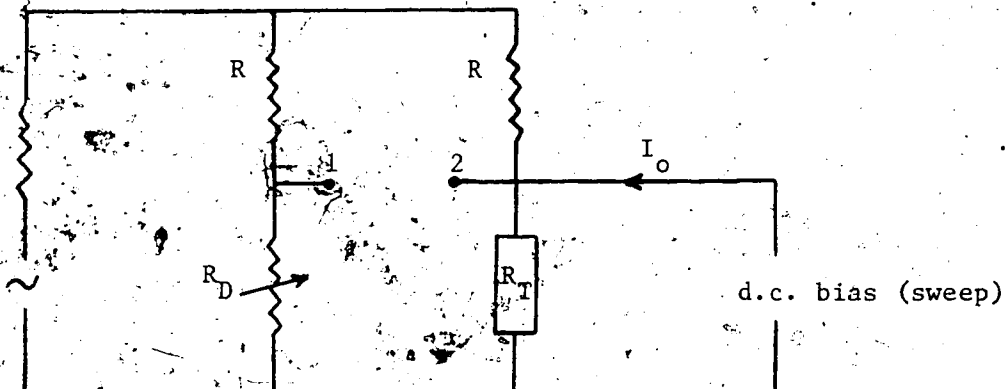


FIGURE 8
CONSTANT CURRENT BRIDGE (and support systems)

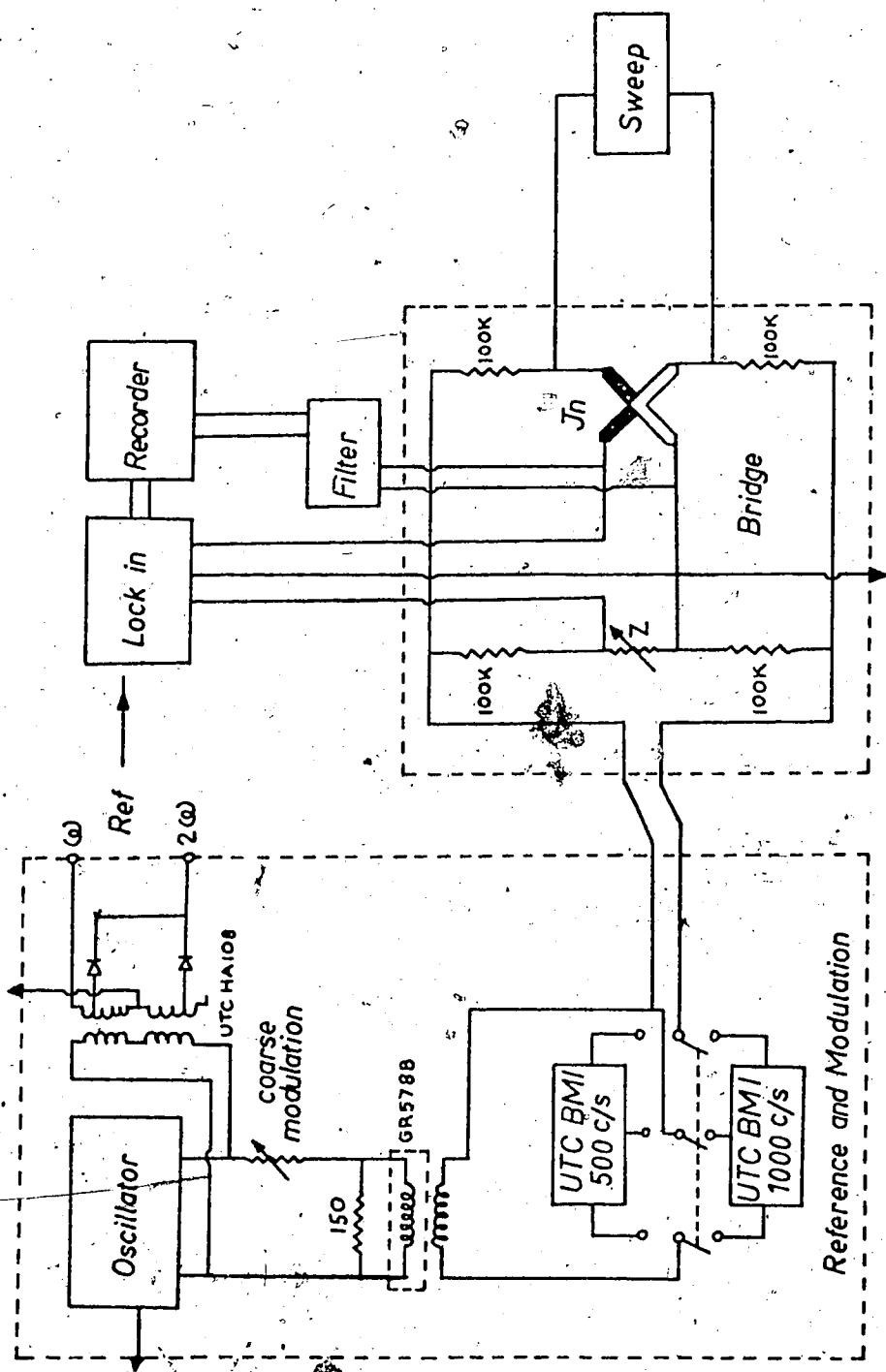
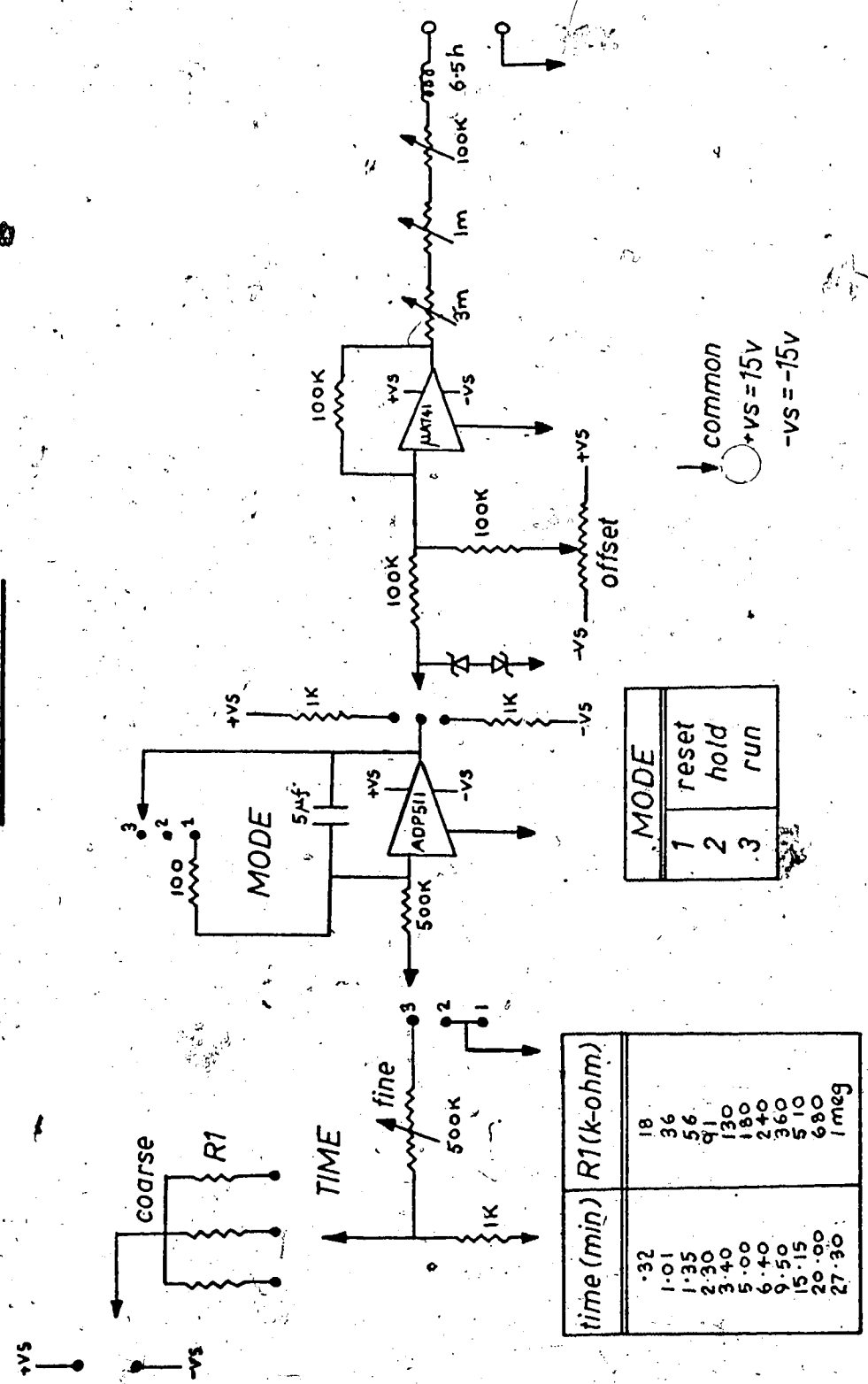


FIGURE 10

SWEEP CIRCUIT



If the current in each arm of the bridge is $\delta \cos \omega t$ then

$$V_1 \approx R_D \delta \cos \omega t$$

$$V_2 \approx I_0 R_D + \left(\frac{dV}{dI} \right)_{I_0} \delta \cos \omega t + \frac{1}{4} \left(\frac{d^2V}{dI^2} \right)_{I_0} \delta^2 (1 + \cos 2\omega t) + \dots$$

where $R_D = R_T$ at balance. Thus:-

$$V_{12}(\omega) = \delta \left[R_D - \left(\frac{dV}{dI} \right)_{I_0} \right] \cos \omega t$$

We see therefore that detecting V_{12}^{ω} is in fact measuring the required quantity $dV/dI = \sigma$

Furthermore it can be seen that the bridge response is linear as would be expected in a passive device. This bridge is claimed by its authors to be able to measure resistance changes of a few parts in 10^5 .

Calibration of the characteristics obtained can be achieved by replacing R_T by a standard variable resistance.

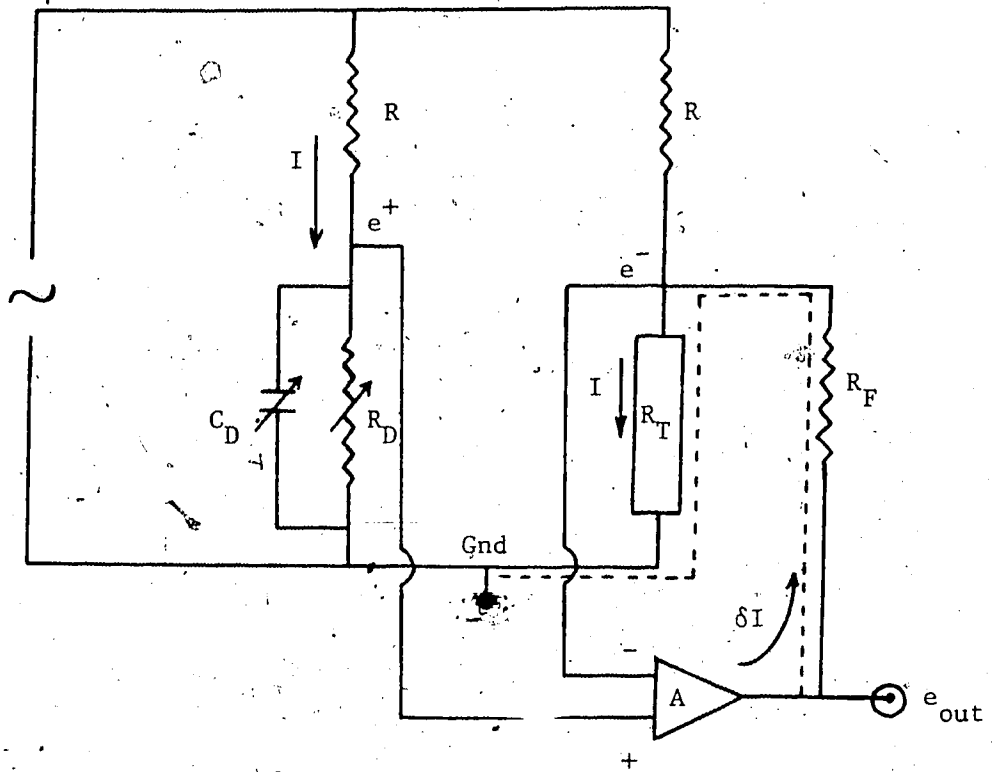
5. The Constant Voltage Bridge

This circuit is of the active variety and actually measures conductance as opposed to resistance. A high gain operational amplifier is used to provide the necessary inversion to do this. A fraction of the output voltage, α say, is fed back so as to maintain a zero signal condition at the input subject to the condition that $\alpha A \gg 1$ where A is the gain.

Conductance measurements of a few parts in 10^5 are obtainable to

an accuracy of 1% and the response of the circuit is linear to .1%. Since the circuit contains an active component a proof of its linear response is given.

The constant voltage bridge may be represented in simplified form as shown below.



By definition

$$e_{out} = Ae_{IN} = A(e^+ - e^-) = A(IR_D - IR_T - \delta IR_T) \tag{4-3}$$

According to the dotted path to ground we can see that

$$e_{out} = \delta IR_F + (I + \delta I)R_T = \delta I(R_F + R_T) + IR_T \tag{4-4}$$

equating 4-3 and 4-4 gives after simplification

$$\delta I = I \left(\frac{R_T(-1-A) + AR_D}{R_F + R_T + AR_T} \right)$$

4-5

Extracting a factor $\beta \equiv R_T/(R_F + R_T)$ we can write 4-5 as:-

$$\delta I = \frac{\beta A}{1 + \beta A} \left(\frac{-1}{A} - 1 + \frac{R_D}{R_T} \right) I$$

4-6

If the feedback resistor R_F had a value of 10^5 ohm with the amplifier gain being $\approx 10^5$ then for tunnel junction resistances $R_T \geq 10$ the prefactor in equation 4-6 is approximately unity. Thus neglecting the small quantity $1/A$ and writing the tunnel conductance $1/R_T$ as G_T we have

$$\delta I = I [R_D G_T - 1]$$

4-7

substituting into equation 4-4 and simplifying yields:-

$$e_{out} = (IR_D R_F) G_T + I(R_D - R_F)$$

4-8

Clearly therefore the output of this bridge is also linear in response but this time in conductance. To calibrate the curves obtained, two points only are required. The most convenient points being those obtained in an open circuit condition (zero conductance) and at the balance condition where $G_T = 1/R_D$.

The condition imposed upon allowable sample resistances by R_F and A were well satisfied in the experiments performed.

CHAPTER 5

EXPERIMENTAL METHOD

1. Sample Fabrication

Prior to the fabrication of the tunnel junction itself, alloys containing various known atomic concentrations of indium in lead were produced in a cleaned environment from extremely high purity constituents (69 purity) which were supplied commercially (Cominco Co.). The tunnel junctions formed from these alloys were of the traditional metal-insulator-metal type prepared by vacuum deposition. Aluminium was chosen for the second electrode for two main reasons. First, it does not itself exhibit any appreciable structure which might cloud observation of the alloy in the energy range of interest and second, it oxidises readily thereby providing a very convenient method of producing the insulating barrier.

A 1" by 1/4" section was cut from a standard glass microscope slide and after being cleaned and fire polished was mounted in the sample holder previously described. This provided the substrate for the tunnel junction and from this point onward it was never necessary to touch the slide again. The sample holder was then constrained in a jig while indium metal contacts were applied to the surface of the glass in places predetermined by the evaporator geometry. Six such contacts were made and wired to the amphenol plug in order to allow four terminal measurements to be made on two junctions simultaneously.

The sample holder was placed in the evaporator which was

pumped to a pressure of better than 1×10^{-7} torr before depositing the aluminium electrode from a multistranded tungsten filament. The sample was then removed from the evaporator and placed in a Fisher Isotemp oven in order to form an oxide layer on the aluminium. Oxidation temperatures used ranged from 100°C to 130°C and were applied for durations of from 1 minute to 5 minutes. This resulted in final tunnel resistances of from 50 ohm to 300 ohm. Several attempts were made to control the oxidation process within the evaporator, one of these consisting of a glow discharge in low pressure oxygen and while the glow discharge method was very reproducible the oxide layers so produced did not in general survive the application of pressure. Having returned the sample to the evaporator, the alloy electrodes were deposited using a molybdenum boat. Both the alloy and aluminium electrodes had an approximate width of $1/16''$ with the latter running the length of the substrate.

2. Mounting Procedure

After filling the oil seal, a slow steady stream of helium gas was allowed to pass through the compressor to the experimental area. Simultaneously the electronic detection system was readied for an immediate check on tunnel resistance. The sample was then removed from the evaporator and, subject to a satisfactory visual inspection of the films, was plugged into the specially designed housing whereupon it was possible to check instantly the approximate tunnel resistance. This was achieved by presetting the modulation level for

a nominal 100 ohm sample and noting the change upon sample contact. The bomb was then screwed loosely into place while being flushed with helium during which time a more accurate check of the tunnel resistance was made.

After tightening the bomb into place the helium pumping chamber was secured (as shown in figure 4) and thermometer connections established. The vacuum can was then soldered into place using Woods metal and evacuated to a pressure of approximately 10^{-5} torr at which point the system was cooled to liquid nitrogen temperature. Pumping of the system was then continued to the lowest attainable pressure in order to provide good thermal isolation between the cryogenic fluid and the bomb.

3. Validity Checks

Before collecting all of the data required from a sample, certain checks were made both on the sample itself and the system. At liquid nitrogen temperature a tunnel characteristic was recorded for $E = + 30$ meV to $E \approx - 30$ meV in order to check for major abnormalities and noise levels. Pressure approaching that used for actual measurements was then applied while monitoring the zero bias resistance of the sample to establish reproducibility in this respect. In addition this provided a check on the pressure system itself including the feedthrough. Between the cool down from liquid nitrogen to liquid helium temperatures, the needle valve operation was checked. The transition temperature was also recorded during this process.

The sample was then further cooled to the ultimate limit attainable and examined for the existence of the localised mode. This was most easily resolved by observing the second derivative curve d^2V/dI^2 . At this temperature the resistance in the gap region at zero bias was checked in comparison to its normal state value. Since by requiring that this ratio be $<10^{-3}$ at $\sim 1K$ we can safely neglect any non-tunnelling contribution to the current.

4. An Experimental Run

Having established the validity of a given sample and that support systems were operating efficiently the various temperature zero pressure characteristics of the sample were recorded. The cryostat was then left until the level of the He_4 bath was just below that of the vacuum can. It was usually found that this practice resulted in a temperature slightly in excess of that predicted by the Simon equation (1937 and 1953) for working pressures of approximately 50,000 p.s.i.g. During the actual pressurisation process, heaters around and inside the pressure tubing were used to insure against capillary blockage. Monitoring of the zero bias tunnel resistance as a function of pressure was also carried out at this time for the prime purpose of determining the final frozen in pressure although it was also possible to detect the occurrence of capillary blockage since when this occurred the external pressure rose while the sample resistance remained constant.

Freezing at constant pressure was then achieved by opening the needle valve while simultaneously maintaining the external pressure

at a constant value. In view of the location of the 1K cooling stage it was expected that the solid would form from the bottom of the bomb upward.

On the occasions when both junctions on the same substrate were useable it was possible to determine the pressure at two points in the solid separated by $\approx \frac{1}{2}$ ". The pressure variation over this distance was found to be of the order of 1% and greatly supports the belief that the technique used did in fact produce pressures which were hydrostatic. With the sample now suspended in solid helium at constant pressure, the liquid helium was restored to a level several inches above the indium O ring seal and the cryostat allowed to cool to the region of 1K, at which point the finite pressure characteristics were recorded.

The penultimate stage of each experimental run provided the challenge of releasing the pressure without destroying the sample and the wiring. It was naturally not possible to attain the temperature necessary to do this while the level of the helium was high and so heaters were employed to boil off the helium to a level below the can. Heat was then applied to the bomb and the high pressure capillary. When the temperature reached a value just below that at which freezing in occurred, the external pressure was raised to just above the frozen in pressure and heating continued. When the fluid phase was realised the pressure indicated by the Heise Bourdon gauge showed a sudden change in value corresponding to the equalisation of pressures. This change was also noted at the sample itself via the zero bias resistance. Early attempts to

release the pressure at temperatures slightly above the melting temperature resulted in destruction of both sample and wiring. This was thought to be due to the retention of a plug of solid helium high in the capillary tube which itself is evidence that the cryostat temperature is non uniform during this process.

An alternative method of de-pressurisation would be to wait until the helium level fell naturally to the desired level but since the cryostat must be full during the actual measurements, this would always be an extremely lengthy wait. In contrast, the method used involved the use of elevated temperatures, a disadvantage which was tolerated subject to the careful monitoring of the process.

After returning the system pressure to zero again a further check on the reproducibility was made both on the resistance value and the observed structure location.

5. Determination of Sample Composition

Despite the fact that the sample was formed from an alloy whose composition was known, the final composition of the evaporated electrode remained to be determined since the vapour pressures of the elements differ widely (see for example Nesmayanov (1963)). To do this, residual resistance ratio techniques were employed (see for example Rosenberg) in which the ratio R_{293}/R_4 for the samples was compared to a calibration curve of the same quantity that had been obtained by measuring a series of alloys of known composition.

Several pieces of each known alloy were taken from various places

on the ingot and rolled out to $\approx .001$ " in thickness. The same sample holder that was used for the tunneling measurements (figure 5) was used to mount these specimens but with a slight variation. A plain glass slide was first placed in the holder and four indium contacts were soldered across its width. Wires were then attached to these contacts at the edges and also to the plug. Pieces of the rolled ingot were then cut to slightly less than the size of this glass slide and placed on top in such a way as to cover the raised indium contacts. A second slightly smaller glass slide was then placed on top (thereby sandwiching the sample onto the contacts) and held in place with masking tape.

The sample holder was then placed in a dipstick arrangement wired for a four terminal resistance measurement. Resistance measurements were then made using a Cambridge Instruments high resolution potentiometer both at room temperature and at liquid helium temperature. The latter measurement was made by placing the sample at the centre of a Westinghouse 21 Kilogauss superconducting magnet and applying the necessary field to induce the normal state. All measurements were carried out for currents in both directions and averaged over all samples from an ingot of a particular concentration. It was in fact found in this way that the original alloys were homogeneous. The calibration curve obtained by this procedure is shown in figure 11.

A determination of the ratio R_{293}/R_4 for the pure lead from which the alloys were made yielded a value of $\approx 21,000$ thereby

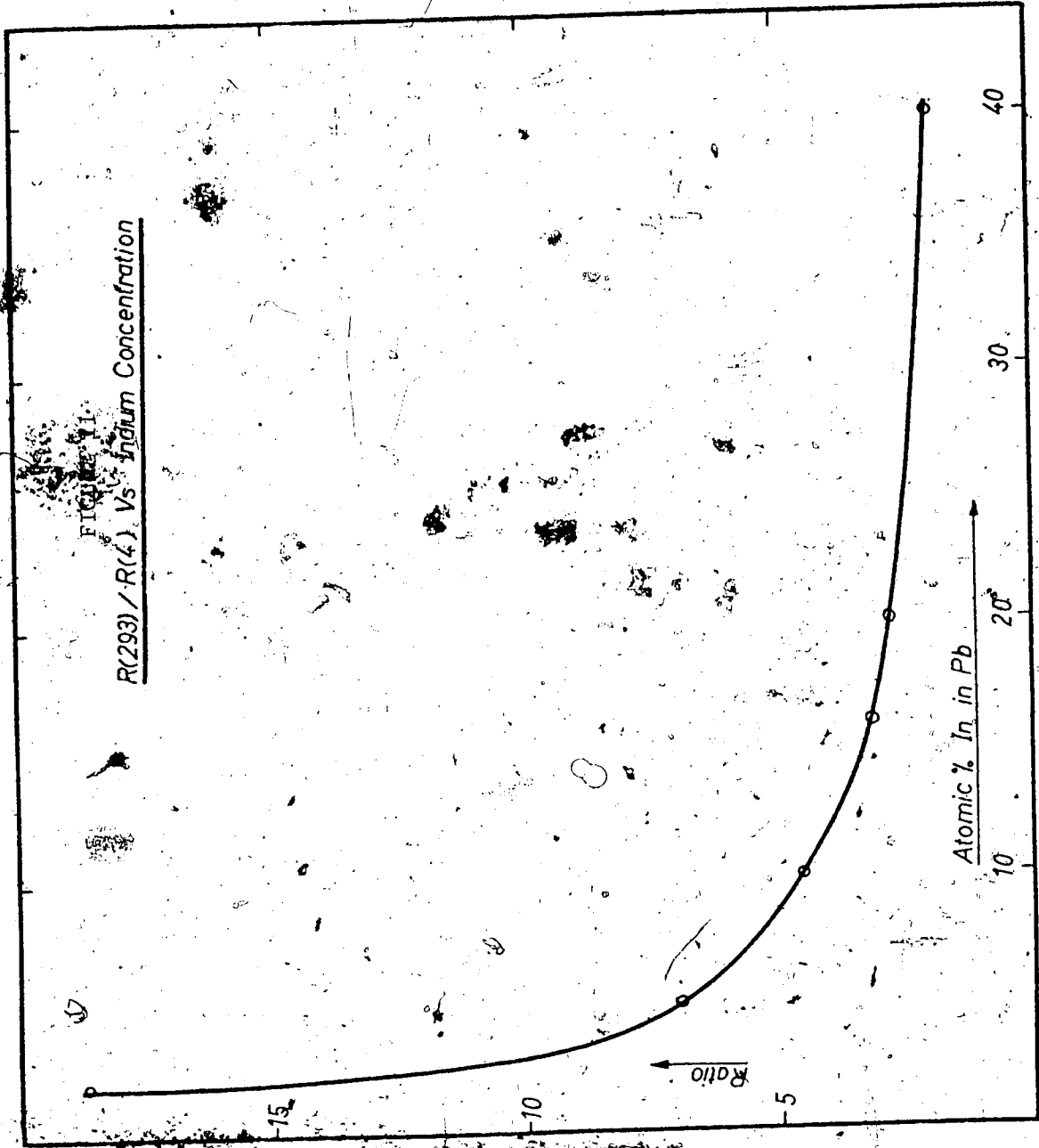
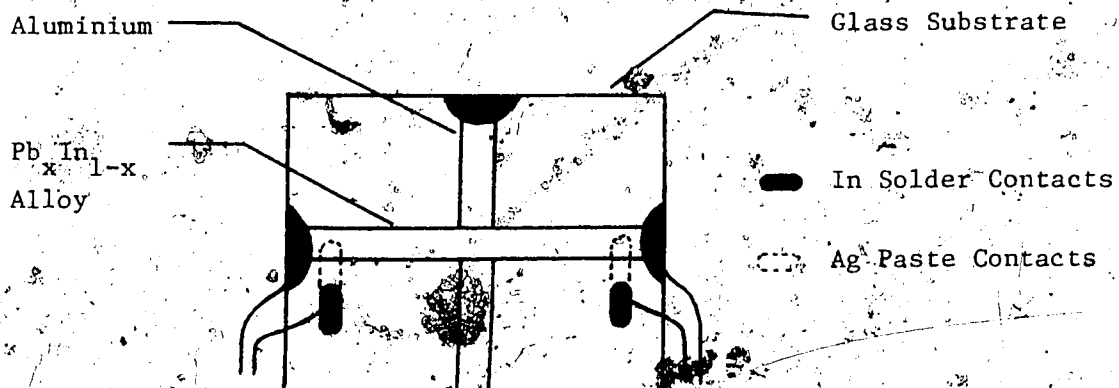


FIGURE 11
R(293) / R(4) Vs. Indium Concentration

Ratio

Atomic % In. in Pb

attesting to its high degree of purity. Before the ratio R_{293}/R_4 for the actual films that were tunnelled through could be determined it was necessary to apply two more contacts to the film to enable a four terminal resistance measurement. This was done as shown in the diagram below which shows an enlarged view of one tunnel junction.



Indium was first deposited at two places as close as possible to the existing contacts and wires attached. Bridges between these points and the film itself were then formed using silver paste. Several such coats of silver paste resulted in very low resistances from A - B of the order of a fraction of an ohm. Once again the same sample holder was utilised. Indium metal was chosen throughout for contacting purposes due to its ability to "wet" glass, however, for this particular application it was essential not to attempt to solder to the film itself with indium since not only would the film probably not survive the process but more importantly if it did, it would not

be possible to say with any certainty that indium from this source had not itself diffused into the film. Contacts using silver paste alone to secure the wires were tried but found to be unreliable at low temperature.

It was very reassuring to notice during these experiments that the potential difference across the alloy films vanished (as would be expected) as the superconducting state was realised regardless of the nature of the contacts.

CHAPTER VI

EXPERIMENTAL RESULTS AND DISCUSSION

1. Introduction

It has been observed by several workers (see Adler (1967) for example and Sood (1971)) that the major properties of interest do not differ significantly over samples whose impurity concentrations vary by ~2 at % which, coupled with the inability of a large proportion of the samples to withstand high pressure, led this author to limit investigations to the concentrations $Pb_{64}In_{36}$ and $Pb_{88}In_{12}$. Such a choice offers the advantage of being able to group together data from samples whose impurity concentrations vary by the above mentioned tolerance (2%) while still being indicative of any trends in the data which are concentration dependent (as a consequence of the ~25 at % difference). Except where specifically mentioned therefore, results quoted henceforth indicate averages for the particular compositions over those samples whose concentrations (as determined by the residual resistance ratio methods described earlier) satisfied the above conditions.

The capacitance of each sample was determined in order to estimate the thickness of the oxide layer (which constituted the barrier). These values ranged from $0.038\mu F$ to $0.051\mu F$ over nine samples which included both the $Pb_{88}In_{12}$ and $Pb_{64}In_{36}$ samples (since the oxide layer is dependent only on the oxidation conditions of the aluminium electrode which is common to both alloys). Assuming

the tunnel junctions to be simple parallel plate capacitors of area $2.25 \times 10^{-6} \text{ m}^2$ and obeying the relationship $C = \epsilon A/d$, the barrier thickness is estimated to be $\sim 50 \text{ \AA}$ where the dielectric constant of the Al_2O_3 has been taken as 9.34 from Gray (1972).

By measuring the resistance of the alloy electrodes (which were of the order 1.5 ohm - .2 ohm) and assuming the value of $21 \mu\text{ohm cm}$ for the resistivity of lead, as taken from Meaden (1965), the thickness of the alloy electrodes is estimated to be from 4400 Å - 5800 Å .

2. Pressure Dependence of the Transition Temperature

The development of the energy gap in the electronic quasiparticle density of states of the superconducting electrode of the tunnel junctions provided a very convenient method of determining the transition temperature of the alloys under investigation. This method involved monitoring the tunnel conductance of the samples at zero bias (in the middle of the energy gap region) and noting the temperature at which the sample conductance exhibited a sharp decrease. Although the width of the superconducting transition has been shown by Adler et al (1965) to be $\sim 5 \times 10^{-2} \text{ K}$ for the lead-indium alloy system (up to 26 at % In), the transition temperatures measured in this way are still very accurate (better than $\pm 10 \text{ mK}$). This is so since the conductance undergoes a very large change over this temperature and is readily observable with the high gain detection system that was employed for the whole of

the annealing experiments performed.

The measurement of the transition temperature for each sample was repeated at least five times and averaged. Experimental accuracy of this data was limited mostly by the resolution of the electronic circuitry associated with the germanium resistance thermometer and to a lesser extent by the uncertainty in the pressure determination.

Included in Table 1, which contains the numerical averages obtained, are average values for the ratio of room temperature resistance to liquid helium temperature resistance of the alloy films (R_{293}/R_4) for the respective compositions. By referring to figure 11 a more precise value for the average sample concentration could be obtained than the nominal 12% and 36 at. % figures which have been rounded to the nearest one percent and which will be used henceforth.

TABLE 1

Pressure Dependence of the Transition Temperature

Concentration (at % In in Pb)	$\frac{R_{293}}{R_4}$	T_c (P=800 p.s.i.) (K)	$\frac{dT_c}{dp}$ ($10^{-5} \text{K bar}^{-1}$)	$\frac{d \ln T_c}{dp}$ (10^{-6}bar^{-1})
12	3.69	7.110 ± 0.008	-3.19 ± 0.16	-4.48 ± 0.22
36	2.18	6.75 ± 0.008	-3.06 ± 0.15	-4.53 ± 0.23

For comparison purposes, Table 2 lists the values of T_c determined by other workers at zero pressure (for impurity concentrations as close as possible to those of interest here).

TABLE 2

Comparative Transition Temperatures (at Zero Pressure)

Authors	Concentration (at % In in Pb)	T_c (P=0) (K)
Adler et al (1967)	12	7.097
Farrel et al (1969)	10	7.05
Farrel et al (1969)	40	6.57
Adler et al (1967)	40	6.63
Wu (1967)	40	6.65*

*Theoretical

Several factors can affect the critical temperature of a superconductor when determined from a thin film sample. The most important of these being effects of structure, impurity content and stress.

For samples which are formed at room temperature the crystalline structure is generally not that different from that of the bulk, providing the film is sufficiently thick, and critical temperatures measured in this case are indicative of those for the bulk material. The transition temperature of superconductors deposited at low temperatures however can exhibit considerable enhancement as for the case of aluminium for which transition temperatures up to 2.5K have been observed. The underlying reason is that at low deposition temperatures the atom mobility of the condensate is low and the crystalline growth is inhibited yielding an amorphous structure. An extreme example of this effect, observed by Lazaren et al (1957)

is that of beryllium which in its normal crystalline state is a non superconductor whilst if deposited at low temperature exhibits a transition temperature of 8K. If annealed, the transition temperature of a sample exhibiting this kind of T_c enhancement reverts to that of the "bulk" state. Since the samples used in these experiments were produced at room temperature and a finite time necessarily elapsed before cooling, structure enhanced T_c 's are not expected.

Impurities constitute a more significant effect on the transition temperature by generally decreasing the value of T_c linearly with decreasing electronic mean free path. According to Mathiessen's rule the decrease in T_c in this regard is linear and given by:-

$$\Delta T_c = K \rho_{res}$$

where K is a constant associated with the solute-solvent pair and ρ_{res} is the residual resistance. Since the samples used were produced by vacuum deposition, the main source of unwanted impurities would be gaseous in nature. Doping of indium with oxygen for example depresses its transition temperature. Depression of the transition temperature due to the inclusion of impurities was minimised however by depositing the films from extremely pure source materials after first attaining the highest possible vacuum. A liquid nitrogen trap was employed to assist in the pumping as well as to reduce the backstreaming of oil from the diffusion pump.

Stress effects as a result of differential contraction between the substrate and the film have the effect of enhancing the transition

temperature. This problem has been investigated by Toxen (1961) for the case of indium on fused quartz substrates who calculated an expression for the change in transition temperature given by:-

$$\Delta T_c = \frac{52}{d} - \frac{750}{d^2}$$

where d is in Angstroms. For a film of thickness 5000Å this amounts to an increase in T_c of ~10mK.

It is difficult to make a quantitative assessment of the net effect of the previous factors although for thick films (>3000Å) bulk values of T_c for lead at least seem to be in close agreement with those obtained using tunnelling techniques (see Franck & Seeler (1967)).

It can be seen from Tables 1 and 2 that there is good agreement between the values obtained here for the alloys with those of other workers. The last column in Table 1 has been included for referral purposes in a later section since it provides a convenient form for theoretical comparison.

The Energy Gap and its Dependence on Pressure

Determination of the superconducting energy gap was less direct than was the determination of the transition temperature. At the finite temperatures employed here, the conductivity does not exhibit a sharp discontinuity at biases close to the energy gap region but appears as a smooth continuous function. Consequently a criterion has to be established for deciding at which point to

evaluate the gap. Figure 12 shows typical characteristics of a $\text{Pb}_{64}\text{In}_{36}$ junction both at low and high pressure recorded at a temperature of $\sim 2.5\text{K}$ in which it can be seen that although a large decrease in conductance occurs, no one obvious point is in evidence for the gap determination.

One such criterion which is widely used is that proposed by McMillan & Rowell (1969) for example in which one makes the measurement from zero applied bias to the mid-point of the current jump in the current voltage characteristic of the superconductor. On the conductance curves that were recorded here this point corresponds to the inflection point on the low energy side of the conductance maximum.

The normalised conductance of a B.C.S. superconductor at finite temperatures has been tabulated by Bermon (1964) as a function of the reduced parameters (bias/energy gap) and (energy gap/ $k_B T$) where k_B is Boltzman's constant and T the temperature in Kelvins. By comparing the conductance plots obtained in these experiments with this tabulation and identifying the one which most closely approximates the experimental curve the value of the latter reduced parameter was identified and since the temperature of the experimental determination was known, it was possible to calculate the gap. In employing this procedure, emphasis was placed on the curve matching procedure in the higher energy region where the gap edge might be expected and where the error in the conductance measurements was least. The criterion of McMillan and Rowell is implicit in this approach if, when the parameter